

Preparation of gold nanoparticles using oxidized polysaccharides

Ing. Alžběta Důbravová, Ph.D.

Doctoral Thesis Summary



Tomas Bata University in Zlín

Centre of Polymer Systems

Doctoral Thesis Summary

Příprava nanočástic zlata pomocí oxidovaných polysacharidů

Preparation of gold nanoparticles using oxidized polysaccharides

Author: **Ing. Alžběta Důbravová, Ph.D.**

Degree programme: Nanotechnology and advanced materials (P3972)

Degree course: Nanotechnology and advanced materials (3942V006)

Supervisor: doc. Ing. et Ing. Ivo Kuřitka, Ph.D. et Ph.D.

Consultant: Mgr. Jan Vícha, Ph.D.

Reviewers: prof. Mgr. Jana Kukutschová, Ph.D.
prof. Mgr. Aleš Mráček, Ph.D.

Zlín, February 2024

© Alžběta Důbravová

Published by **Tomas Bata University in Zlín** in the Edition **Doctoral Thesis Summary**.

The publication was issued in the year 2024.

Key words in Czech: *celulóza, kyselina hyaluronová, dextran, alginát, selektivní oxidace, katalýza, Povrchově vylepšený Ramanův rozptyl, kompozitní materiály*

Key words: *cellulose, hyaluronic acid, dextran, alginate, selective oxidation, catalysis, Surface-enhanced Raman scattering, composite materials*

Full text of the doctoral thesis is available in the Library of TBU in Zlín.

ISBN 978-80-7678-239-6

ACKNOWLEDGEMENT

First of all, I would like to thank my supervisor, Assoc. Prof. Ing. et Ing. Ivo Kuřitka, Ph.D. et Ph.D., for all the help, support, professional guidance, advice, and experience given throughout my studies.

Next, I would also like to express sincere gratitude to my consultant, Mgr. Jan Vícha, Ph.D., for his valuable advice in setting up experiments and evaluating results. I would also like to thank him for his patience, time, and all the knowledge he shared with me.

Many thanks also to Ing. Lukáš Münster, Ph.D., for his time, all advice and tips and especially for his help in the laboratory.

I would also like to thank my colleagues at the Centre of Polymer Systems for their help with the experimental work and their moral support throughout the study. Here, special thanks especially go to Mgr. David Škoda, Ph.D., Ing. Monika Muchová and Ing. Kateřina Štěpánková. I would also like to thank Kristýna Valášková from Prof. Humpolíček's group for performing antibacterial tests on the composite materials and also Ing. Lenka Lovecká, Ph.D. from Dr. Kimmer's group for her tireless preparation of the fibre bodies.

Finally, I would like to thank all my family, friends, and husband for their patience, for tolerating my moods while writing my dissertation, for the supply of chocolates and, on the whole, for moral support throughout my studies.

The dissertation was also supported by IGA projects, namely IGA/CPS/2020/003, IGA/CPS/2021/002, IGA/CPS/2022/002 and IGA/CPS/2023/006. Projects RP/CPS/2020/006, RP/CPS/2022/007, and Grant GA23-07361S also contributed. I want to thank the Centre of Polymer Systems and the Tomas Bata University in Zlín for financial support during my studies.

ABSTRACT

This work focuses on preparing gold nanoparticles (AuNPs) using selectively oxidized polysaccharides and evaluating their application potential. In the first step, polysaccharide derivatives were prepared by selective oxidation and subsequently characterized. The AuNPs were synthesized using the prepared materials after optimizing the reaction conditions and then characterized in terms of structure and in terms of stability and gold/polysaccharide content. Subsequently, the application potential for catalytic and SERS effects was studied. In the next step, a composite material of chitosan nanofibers and DAC-decorated gold nanoparticles was prepared by exploiting the Schiff base formation between the carbonyl groups in the AuDAC shell and the amine groups in the chitosan nanofibers. The bond was subsequently stabilized using sodium borohydride. The composite material was characterized in terms of structure, stability, and composition and the application for the catalytic reduction of 4-NP to 4-AP was tested. Based on the promising results of the AuDAC nanoparticles, AuNPs were also prepared using other dialdehyde polysaccharides. They all showed a more efficient catalytic reduction of 4-NP than the AuDAC. Subsequently, it was confirmed that the proposed formation of composite bodies applies to different types of AuNPs and different nanofibers containing amine groups. Finally, antibacterial activity was also tested on these bodies.

ABSTRAKT

Tato práce se zabývá přípravou zlatých nanočástic (AuNPs) pomocí selektivně oxidovaných polysacharidů a stanovení jejich aplikačního potenciálu. V první fázi byly pomocí selektivní oxidace připraveny deriváty polysacharidů a následně byly charakterizovány. Pomocí připravených materiálů byly následně syntetizovány AuNPs, kdy proběhla optimalizace reakčních podmínek a následně charakterizace z hlediska strukturního a z hlediska stability a obsahového zastoupení složek zlato/polysacharid. Studován byl následně aplikační potenciál pro katalytické účinky a pro SERS efekt. V dalším kroku byl připraven kompozitní materiál z chitosanových nanovláken a roztoku zlatých nanočástic připravených pomocí DAC, kdy došlo k využití tvorby Schiffovy báze mezi karbonylovými skupinami ve slupce AuDAC a aminovými skupinami v nanovlákněch z chitosanu. Vazba byla následně stabilizována pomocí borohydridu sodného. Kompozitní materiál byl následně charakterizován a proběhla i jeho zkouška aplikovatelnosti pro katalytickou redukci 4-NP na 4-AP. Na základě slibných výsledků AuDAC nanočástic byly připraveny i AuNPs s využitím dalších dialdehydů polysacharidů. Všechny prokázaly efektivnější katalytickou redukci 4-NP ve srovnání s AuDAC. Následně bylo potvrzeno že výše navržená tvorba kompozitních těles je využitelná pro různé typy AuNPs a různé typy nanovláken obsahující aminové skupiny. Na závěr byla testována i antibakteriální aktivita u takto připravených kompozitních těles.

TABLE OF CONTENT

ACKNOWLEDGEMENT	3
ABSTRACT	4
ABSTRAKT	4
TABLE OF CONTENT	5
1. INTRODUCTION	7
2. NANOPARTICLES	7
2.1 Gold nanoparticles	7
2.1.1 Applications	8
2.1.2 Nanoparticle stability	9
2.1.3 Preparation	11
3. POLYSACCHARIDES	12
3.1 Cellulose	12
3.2 Hyaluronic acid	12
3.3 Chitin and chitosan	13
3.4 Dextran	13
3.5 Alginate	14
3.6 Regioselective oxidation	14
4. COMPOSITES	16
4.1 Polyamide	16
5. AIMS OF DOCTORAL THESIS	17
6. EXPERIMENTAL PART	18
6.1 Preparation of samples	18
6.1.1 Selectively oxidized polysaccharides	18
6.1.2 Gold nanoparticles	18
6.1.3 Preparation of composite material from AuDAC and chitosan nanofibers.....	19
6.1.4 Preparation of composite mats from AuDAC, AuDAH, chitosan and PA nanofibers	20
6.2 Characterization of samples	20
6.3 Catalysis	20
7. RESULTS AND DISCUSSION	22
7.1 Preparation and characterization of polysaccharide derivatives	22

7.2 AuNPs from dicarboxy polysaccharides.....	23
7.2.1 Reduction mechanism	24
7.2.2 SERS application.....	25
7.2.3 Catalytic activity.....	26
7.3 Screening study of AuNPs from dialdehyde cellulose	27
7.4 AuDAC and chitosan nanofiber composite	28
7.4.1 The catalytic activity of AuDAC and composite material	29
7.5 Catalytic activity of AuDAH, AuDAAL and AuDADXA.....	30
7.6 Composite materials from AuDAC, AuDAH, chitosan and PA nanofibers	31
CONCLUSIONS	33
CONTRIBUTION TO SCIENCE AND PRAXIS	35
REFERENCES	36
LIST OF FIGURES	45
LIST OF TABLES	46
LIST OF ABBREVIATIONS AND SYMBOLS.....	47
LIST OF PUBLICATIONS.....	48
CURRICULUM VITAE	49

1. INTRODUCTION

Among metallic nanoparticles, gold nanoparticles have attracted the attention of many scientific groups, especially for their remarkable optical and electrical properties and for the possibility of modifying their surface [1]. This has led to a shift from their original use as an inorganic dye thousands of years ago to applications in many sectors such as biomedicine, the pharmaceutical and food industries, chemical catalysis, etc. The uses of gold nanoparticles are linked to specific properties closely related to their size, shape, structure, and surface composition [2]. These parameters can best be influenced during the preparation of AuNPs. The growing interest in developing environmentally friendly synthetic methods has led to the development of methods replacing toxic organic solvents with non-toxic, biocompatible, and biodegradable substances. This has led to syntheses based on polysaccharides that can reduce gold salts while stabilizing the resulting nanoparticles [3, 4]. Despite promising results, the exact relationship between the properties and structure of the polysaccharide and the resulting AuNPs is poorly understood, complicating their targeted preparation. Moreover, the properties of native polysaccharides, such as molecular weight, number of functional groups, and degree of branching, often vary according to their biological source and processing method, further complicating control over the properties of the prepared nanoparticles. Therefore, controlled modifications of polysaccharides with well-defined properties are proposed as a suitable alternative for synthesizing gold nanoparticles, which will be addressed in this work. One such modification is the regioselective oxidation of polysaccharides to dialdehyde- or dicarboxy- derivatives with controllable molecular weight [5–8].

2. NANOPARTICLES

The nanoparticles are one of the sub-groups of nanomaterials that are characterized by their dimensions falling within the interval from sub-nanometres to hundred nanometres [9]. These sizes give completely different physical properties to the nanomaterial in comparison with the material of the same composition but in bulk size. For example, nanomaterial crystals have a lower melting point compared to their bulk form because most of the atoms and ions in the nanomaterial are surface atoms and ions, which affects the surface energy of the material and, thus thermal stability [2]. Due to these unique properties, nanomaterials have gradually found applications in several fields, such as medicine, food industry, electronics, molecular biology, and pharmacy [10]. In this thesis, I will focus on one very specific type: gold nanoparticles (AuNPs) [2, 10].

2.1 Gold nanoparticles

Gold nanoparticles have different properties compared to bulk gold, i.e. a non-reactive noble element. Nevertheless, they have been used for a long time,

although in their early days, they were mainly for decorative purposes [11, 12]. Since then, however, their preparation process has gradually evolved and improved, leading to a wider range of applications in more areas, where they could apply their properties. Some of these significant features include interesting electronic and optical properties, which depend on their shape and size [13, 14]. Due to this dependence, there is also a change in the colour of the nanoparticle solution, which is caused by a phenomenon called localized surface plasmon resonance (LSPR), see Figure 1 [15, 16]. Furthermore, they have a high surface area to volume ratio, and one of the advantages is also the possibility of modifying this surface using materials with functional groups such as amines, thiols, and phosphines [11].



Figure 1: Display of AuNPs colour dependence on their size and shape [12, 15]

2.1.1 Applications

AuNPs of different sizes and shapes and homogeneous and heterogeneous compositions have been prepared by different preparation methods and variances of synthesis conditions [2, 17, 18]. Thanks to its diversity, AuNPs are used in several fields.

2.1.1.1 Medicine and pharmaceutical applications

One of the possible applications of AuNPs is in medicine. Nanoparticles with very small diameters can penetrate cells and cellular compartments but are also very toxic. However, these properties can be exploited in clinical therapies if targeted to malignant or diseased tissues. Another interesting property that can be used in this field is the ability to absorb light and convert it into heat. This can be used, for example, to destroy cancer cells, viruses, or bacteria [12]. Thanks to their antioxidant and anti-inflammatory effects, they also find applications in wound healing, especially on the skin. Whether it is nanoparticles alone or a composite with another material such as chitosan, polyvinyl alcohol, or bioactive glass, all these materials show great promise in this area [19–21].

2.1.1.2 Imaging and sensing techniques

AuNPs can also find their function in various imaging and sensing techniques. For example, gold nanoparticles can increase the efficiency of Raman

spectroscopy due to the so-called Surface-Enhanced Raman Scattering (SERS) effect by several orders of magnitude. This is applied in highly sensitive chemical and bioanalytical sensing and imaging techniques. AuNPs with uneven shapes and irregular surfaces are preferred to spherical nanoparticles in this regard. This is due to the formation of electromagnetic "hot spots" on edges or points of such an uneven surface, greatly amplifying the Raman signal of the molecule being analyzed [22, 23].

2.1.1.3 Catalytic applications

Gold nanoparticles are also known for their excellent catalytic efficiency, which is also dependent on the size and shape of the nanoparticles [24]. For example, nanoparticles of sub-nanometre size give the best results. However, as the size increases, the catalytic efficiency decreases [25]. Examples of reactions that can be catalyzed by AuNPs include the conversion of alcohols to aldehydes, the oxidation of carbon monoxide at low temperatures, or the hydrogenation of nitro groups and alkenes [26]. For example, Abbas and co-workers [27] created a composite material of gold-peptide nanoparticles, which they used to reduce the organic molecule pollutant p-nitrophenol (4-NP) to p-aminophenol (4-AP), a substance used in the production of paracetamol, see Figure 2 [27].

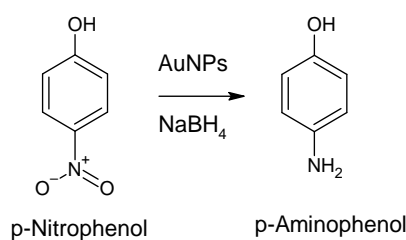


Figure 2: Reduction of 4-nitrophenol to 4-aminophenol in the presence of NaBH_4 and AuNPs [27]

2.1.1.4 Other applications

Due to AuNP's antibacterial and antifungal properties, they also find use in the food industry. Usually as a packaging material, most often in the form of a composite with a polymer [28]. Alternatively, they also serve as detectors, e.g. for the colorimetric detection of hydrazine, as an electrochemical sensor for the rapid detection of food additives, or for the detection of pathogenic bacteria, antibiotics, toxins and heavy metals [29].

2.1.2 Nanoparticle stability

The stability of nanoparticles can be considered from several aspects, with the main issue always being the final use of the material. For some applications, stability may only be required before application, such as in sensors based on colorimetric detection. Conversely, long-term stability is needed for catalysts that can be used in multiple cycles to maintain the same catalytic response throughout the intended use.

From an **aggregation point of view**, it is about preserving the original nanoparticle assembly and thus avoiding collisions. In particular, this phenomenon can be visually observed on noble metals due to their plasmonic properties depending on the distances between the particles [30]. Dynamic Light Scattering (DLS) can then be used for materials to which the plasmonic effect does not apply so that it can be established whether aggregation is occurring [31]. The nanoparticles' stability in solution and, thus, the tendency to aggregate depends on the energies of collisions versus the potential energy, so if the probability of elastic collisions increases, the stability increases. One of the examples of how to ensure this stability is the formation of a mixed monolayer on the surface of nanoparticles. However, this stability can still often be achieved for a specific time, depending on the storage of the material [30, 32].

From a **compositional perspective**, it is a matter of maintaining the chemical identity and crystallinity of the core throughout the experiment or time. Instability in this kind of matter can be caused by oxidation or sulfidation. Since this stability depends on the standard reduction potential of the material, it can be increased for metal/metal oxide nanoparticles by creating a thin outer oxide layer of a more reactive metal [30, 33, 34].

In **terms of shape**, it is about retaining the local structure and radius of curvature at the atomic scale and nanoscale [30]. This stability description is closely linked to the physicochemical properties of nanomaterials and thus affects, in particular, nanoparticles' catalytic and plasmonic properties [35]. Such instability can be caused, for example, by the desorption of capping agents and can thus be prevented by molecular adsorption [30].

In **terms of size**, stability is about keeping the dimensions for the duration of storage or experimentation. Since many properties of metal nanoparticles are closely related to their size, it is necessary to maintain a given size that is most suitable for different applications. The stability of the nanoparticle size depends mainly on the preparation method, their resulting homogeneity, and the content of defects in the structure. The composition and structure of the used stabilizing agent also play a significant role, affecting the formed nanoparticles' surface tension [30, 35].

Stability can also be understood regarding **surface chemistry**, mainly maintaining the original surface potential, structure, and functional surface chemistry. Thus, stability relates to the function of intermolecular forces; this applies to the nanoparticles and their surroundings. Stability can be determined by measuring the zeta potential, which is often dependent on the pH of the solution [30]. Zeta potential is the charge of the nanoparticle in the shear plane, see Figure 3, and its value is related to the surface charge of the nanoparticle. This analysis is used because the surface charge cannot be measured directly due to the

impossibility of completely removing the adsorption of ions on the surface of these particles [31].

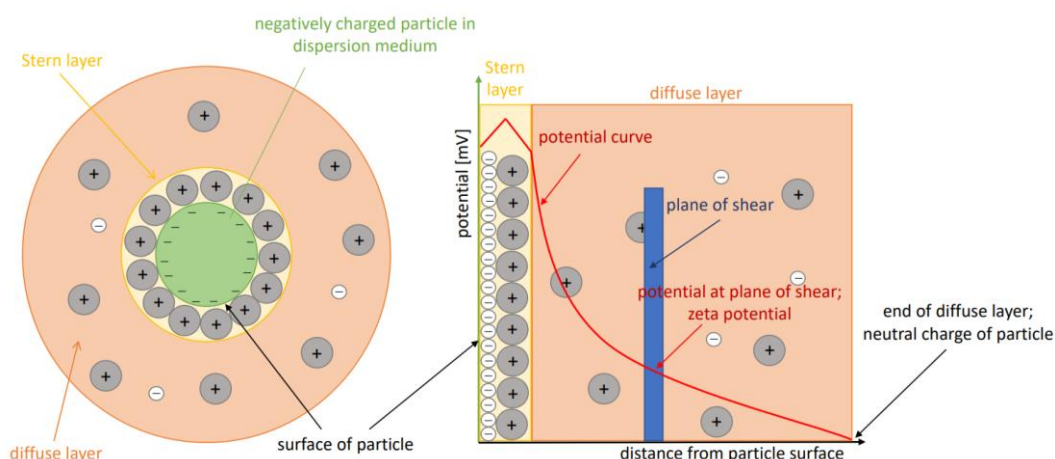


Figure 3: Schematic representation of a particle in a dispersion medium and theoretical scheme of the zeta potential [31]

Properties affecting surface stability are metal oxidation, trace elements, possible surface contamination and defects. An example of how to ensure this stability is the previously mentioned modification of the surface of nanoparticles by steric hindrance or ionic surfactants and antiflocculants [30–32].

2.1.3 Preparation

In general, bottom-up and top-down approaches are used for the preparation of nanoparticles,. An example of a top-down approach might be milling and attrition. However, these approaches lead to a rather inhomogeneous distribution of nanoparticles of different shapes and often cause defects on the surface of the material. In addition, contamination from the milling medium may be introduced into the product material. Therefore, a more widely used method for nanoparticle preparation is the bottom-up approach, which allows the formation of fewer defective nanoparticles and a relatively homogeneous composition. Examples of this approach are homogeneous nucleation, heterogeneous nucleation on substrates, or film deposition [2].

According to the literature, Michael Faraday was the first to describe the synthesis of AuNPs. He found out that carbon disulfide can stabilize the ruby liquid formed in the aqueous reduction of gold chloride by phosphorus. Although there has been a significant shift in synthesis since then, the principle is fundamentally the same. It is the reduction of gold ions, specifically Au(III) salts, taking place in solution in the presence of reducing and stabilizing agents [12, 36]. The most common method, which provides spherical AuNPs in a wide range of sizes, builds on the work of Enustun, Turkevich, and Frens and uses a citrate to reduce the gold salts. The following studies allowed us to understand the dependence of some

phenomena, such as light scattering, Brownian motion, or sedimentation, on the size of the prepared AuNPs [37, 38].

However, in recent years, the trend has been to develop a one-step synthesis that limits the use of toxic substances such as sodium borohydride. Because of this desire, much attention has been focused on syntheses using polysaccharides [39, 40].

3. POLYSACCHARIDES

Polysaccharides are long chains of monosaccharide units interconnected by glycosidic bonds. According to the type of monosaccharide units, they can be divided into homopolysaccharides and heteropolysaccharides. If it is a homopolysaccharide, the material is composed of only one type of monosaccharide. If it is a heteropolysaccharide, the monosaccharide units alternate [41]. The great advantage of polysaccharides is that they are natural renewable resources, often biodegradable, biocompatible, and non-toxic, which makes them appealing for many applications [42].

3.1 Cellulose

Cellulose is classified as a linear polymer and is composed of β -1,4-linked D-glucose units, see Figure 4. Structurally, it consists mainly of highly oriented crystal regions, but amorphous parts can also be found. Due to its strong hydrogen bonding system, its solubility in most solvents is limited [43, 44].

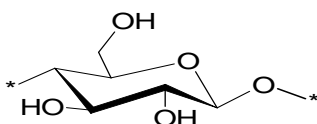


Figure 4: Structure of the cellulose unit [43]

Cellulose has long been associated with paper production; therefore, various plant species logically come to mind as a major source. Besides plants, cellulose can be obtained synthetically from bacteria, fungi, or small animals such as tunicates [45]. In addition to the aforementioned applications in paper and cardboard production, it is also used in biofuels and the pharmaceutical, textile, and food industries [46].

3.2 Hyaluronic acid

Hyaluronic acid (HYA) is a linear polysaccharide consisting of repeating units of D-glucuronic and N-acetyl-D-glucosamine, see Figure 5. It can be found in various strains of bacteria, in chicken combs, and in most vertebrates, where it is abundantly represented in the vitreous of the eye and umbilical cord. HYA is a highly hydrophilic material and negatively charged due to its molecule carboxyl groups. It forms a pericellular coat around most cells, where it regulates cell

adhesion, proliferation, and migration. It is also associated with forming a viscous network at high molecular weights and is essential as a lubricant for joints [47, 48].

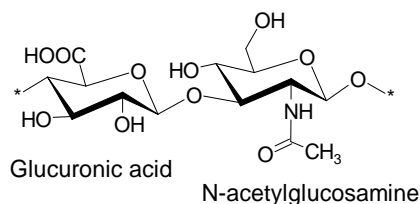


Figure 5: Structure of the hyaluronic acid unit

Hyaluronic acid has applications thanks to its unique properties, especially in the medicine and cosmetic industry. In medicine, it is used, for example, in treating osteoarthritis and wound healing in infectious and oncological diseases. In the cosmetic industry, it plays an important role in solving problems associated with aging processes and aesthetic problems [48, 49].

3.3 Chitin and chitosan

Chitin is an essential component of the exoskeleton of aquatic crustaceans and also part of the cell walls of insects and fungi [50]. Structurally, it is a β -(1 \rightarrow 4) linked 2-acetamido-2-deoxy- β -D-glucan. By deacetylating chitin, chitosan (CHIT), which is its N-deacetylated derivative, can be obtained, see Figure 6. Chitosan forms a less crystalline structure than chitin and is soluble in most aqueous acids [50].

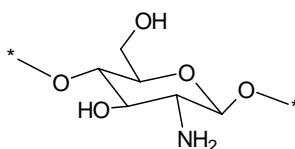


Figure 6: Structure of chitosan unit [50]

Chitosan is a suitable material for the formation of membranes and nanofibers. It is used in the pharmaceutical, food industry, and environmental fields, particularly for its ability to selectively bind various materials such as fats, proteins, and metal ions [42, 51, 52].

3.4 Dextran

Dextran (DXA) is an extracellular polysaccharide consisting of a linear chain of D-glucoses linked by α -(1 \rightarrow 6) bonds, see Figure 7. Branching of D-glucose can also occur by forming α -(1 \rightarrow 4), α -(1 \rightarrow 3) or α -(1 \rightarrow 2) bonds. This polysaccharide is produced mainly by lactic acid bacteria, which can be obtained, for example, from dairy foods, meats, cereals or vegetables [53]. Naturally occurring dextran is amorphous and soluble in various solvents like water, DMSO, formamide or ethylene glycol [54].

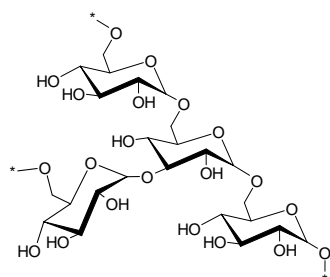


Figure 7: Structure of dextran unit [53]

Thanks to its antithrombotic effect, it is used in the treatment of deep vein thrombosis or postoperative pulmonary embolism. In an aqueous solution, it is used to replace mild blood loss. Another application is in cosmetics and baking, where its moisturizing properties are used. Also, in the aqueous two-phase system with polyethylene glycol, it is used to separate mixtures of biomolecules and subcellular particles [54].

3.5 Alginate

Alginate (AL) is a polysaccharide composed of α -L-guluronic acid and β -D-mannuronic acid blocks linearly linked by 1,4-glycosidic bonds, see Figure 8. Structurally, the blocks in the chain occur individually or in alternating form [55]. Depending on the source, the content of guluronic acid blocks varies, with the material with a higher content of this component finding greater use in biomedical applications due to its low immunogenicity in the body and ease of processing [56]. AL is produced by brown seaweed Algae or bacteria and is soluble in water. Because of its occurrence in anionic form, combined with divalent cations, it leads to the construction of hydrogels [55].

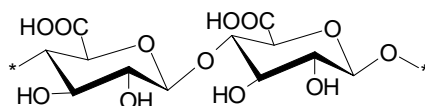


Figure 8: Structure of alginate unit [57]

Due to its interaction with proteins, fats, and fibers, AL finds application in the food industry as a stabilizer and emulsifier. The mixture of alginate and pectin then forms a gelling agent, often used in low-calorie substitute foods. It also finds application as a dental impression material, wound dressing material, or as an excipient in pharmaceuticals due to its biocompatibility and non-immunogenicity [56].

3.6 Regioselective oxidation

Due to their properties, polysaccharides appear to be a suitable material for the one-step green synthesis of gold nanoparticles. In addition to being renewable biocompatible materials, they have the advantage of being able to behave simultaneously as reducing and capping agents. However, it is known that the

resulting shape and size of AuNPs are influenced by the molecular weight of the polysaccharides and the functional groups in their structure [25, 58]. Therefore, it appears more appropriate to use polysaccharide derivatives containing more of these reducing or stabilizing groups than the native polysaccharides for the synthesis of AuNPs.

One possible preparation of such derivatives is the regioselective oxidation of polysaccharides, which can have two stages. The first, primary oxidation uses sodium periodate to oxidize the vicinal -OH groups to -CHO with simultaneous cleavage of the carbon-carbon bond to form dialdehydes of individual polysaccharides, see Figure 9A. These -CHO groups can then react, for example, with the -NH₂ groups of the respective substrates to create a Schiff base, see Figure 9B [59–61]. This is often followed by reduction with NaBH₄, where the imine bonds (C=N) are converted to secondary amine bonds (C-N), and the unreacted aldehyde groups are simultaneously reduced to primary alcohols [61]. This is due to the stabilization of the bond, as the Schiff base is reversible, but the resulting amine bond is not, see Figure 9B and 9C [62].

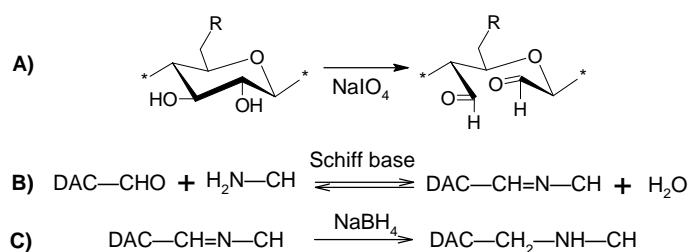


Figure 9: General scheme of primary oxidation (A), formation of Schiff base between CHO and NH₂ group (B) and formation of amine bond after reduction of Schiff base (C) [60, 61]

The primary oxidation can be followed by secondary oxidation using sodium chlorite. This oxidizes the aldehydes and disrupts the hemiacetal groups in the dialdehydes of polysaccharides, and the resulting products of the reaction are dicarboxylates, see Figure 10. In addition, using the sulfonation-induced chain scission method, controlled hydrolysis of dicarboxypolysaccharide chains can be achieved by adding sulfamic acid, allowing better control of their molecular weight [6, 7].

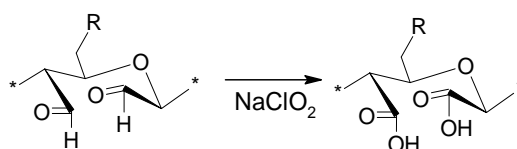


Figure 10: General scheme of secondary oxidation [60]

4. COMPOSITES

Generally, a composite is a material consisting of two or more materials differing in physical, mechanical, or chemical properties. Depending on the volume, distribution of the individual components, and their arrangement as a whole, the resulting properties of the final composite can be influenced. In terms of composition, the composite consists of two phases, namely the so-called matrix and dispersion phase. The matrix is usually a continual phase with relatively high ductility and low fracture strength. According to the dispersion phase, which can be in various forms such as particles, fibers, and sheets, the composites are divided into particle-reinforced, fiber-reinforced, or structural composites [63].

If we focus directly on polymer/metal nanoparticle composites, their applications are extensive. Thanks to their unique properties, such as antimicrobial effect, conductivity, and catalytic activity, they find applications in water purification, sensing techniques, the food and textile industry, medicine, and many more. The advantage of these composites is that only a low concentration of metal nanoparticles, below 10%, is sufficient to improve the final material's properties. The preparation of polymer/metal nanoparticle composites can be divided into *in-situ* methods and *ex-situ* methods [64].

4.1 Polyamide

Polyamides (PA) are thermoplastic polymers containing an amide bond. One type of PA are the aliphatic polyamides called Nylons, which can be formed by a condensation reaction between a diamine and a dibasic acid, ring-opening polymerization of lactam and self-condensation of amino acids, see one example in Figure 11. The number after the name of PA indicates the number of carbon atoms in the monomer. Nylons are semi-crystalline materials, less soluble in solvents, with high heat resistance, good strength, and ductility [65, 66].

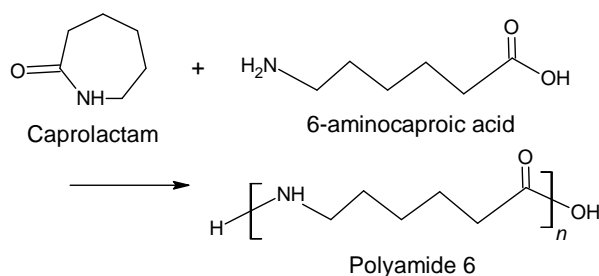


Figure 11: Synthesis of Polyamide 6 [67]

Various PA are used, for example, in the automotive industry due to their toughness, corrosion resistance and lightweightness. PA films and coatings are widely applied as food packaging materials, and aliphatic polyamides are used in pharmaceutical and medical applications for their biocompatibility and biodegradability [68, 69].

5. AIMS OF DOCTORAL THESIS

This work aims to study the preparation and properties of AuNPs prepared using selectively oxidized polysaccharides of different types and different DO.

The aim can be then divided into the following main goals:

- To understand the mechanism of the reduction occurring during the synthesis of AuNPs and the relationship between polysaccharide structure and nanoparticle properties.
- To elucidate the effect of reaction conditions on the final shape, size, and stability of AuNPs.
- To explore the application potential of the AuNPs prepared in this way, especially in the field of catalysis and spectroscopic properties, particularly the SERS effect.
- To test the possibility of deposition/adsorption of such prepared AuNPs on suitable matrices using aldehyde/carboxyl groups on their surface and find out application potential for these composite materials.

6. EXPERIMENTAL PART

6.1 Preparation of samples

6.1.1 Selectively oxidized polysaccharides

DAC, DAH, DAAL, DADXA, DCC, and DCH were obtained by selective oxidation of the source polysaccharides, cellulose, hyaluronic acid, alginate and dextran, respectively. First, **primary oxidation** was carried out, in which polysaccharides reacted with NaIO_4 . The oxidation occurred in the dark and was terminated after a specified time by adding an excess of ethylene glycol. Subsequently, samples were purified, filtered, flash-frozen, and lyophilized. The exception was for the DAC, where solubilization of the material is required for its solubility in water when used as a primary oxidized polysaccharide. After purification, the DAC material was heated in an oil bath, subsequently centrifuged, filtered, dialyzed and then lyophilized.

In the subsequent **secondary oxidation**, the dialdehyde derivatives were oxidized with sodium chlorite in an acidic environment without light. For concentrations of individual substances and other details, see the article [70]. The secondary oxidations were terminated by adding NaOH at pH 8 and then dialyzed against demineralized water. The pH of the resulting solutions was then adjusted to 7.4, followed by filtration and lyophilization. The resulting oxidized polysaccharides DCC, DCC-70 and DCH were obtained in the form of sodium salts.

6.1.2 Gold nanoparticles

The aforementioned polysaccharide derivatives were further used in the synthesis of AuNPs. Optimization of the reaction parameters, namely polysaccharide concentration, reaction time, amount of gold precursor, and pH, was carried out during the synthesis.

In general, for **dicarboxy derivatives**, the procedure involved first dissolving a given amount of polysaccharide in demineralized water, then adding a gold precursor solution and then the desired amount of NaOH. The solution was vortexed and placed in an oil bath heated to 90 °C, where it was shaken for several hours. The resulting gold nanoparticle solution was then filtered and analyzed. The optimization of reaction conditions (reaction time, polysaccharide weight concentration, concentration of NaOH) was performed in three series when only one parameter was changing. These studies were used to identify the most suitable conditions for AuNP preparation, depending on the gold nanoparticles' size, shape, and stability. According to these, production samples were prepared, purified by filtration and repeated centrifugation, and analyzed by available methods.

For **dialdehyde cellulose**, the general procedure involves first dissolving a given amount of DAC in demineralized water. The pH of the solution was then adjusted

to 7 with NaOH and was placed in an oil bath heated to 90 °C and left for tempering. The desired amount of gold precursor was added, and the solution was vortexed. Finally, the amount of NaOH was also added and vortexed again. The formation of AuDAC nanoparticles was instantaneous, so immediate cooling in a water bath in a refrigerator was carried out, followed by product analysis. The optimization of reaction conditions (weight concentration of DAC, weight concentration of gold precursor, concentration of NaOH) was performed in three series when only one parameter was changing. These studies were used to select the most suitable conditions for AuNP preparation, depending on the gold nanoparticles' size, shape, and stability. According to these, the production sample was prepared and, for further processing, was stripped of residual gold salts by dialysis against dilute HCl solution at pH 3.5.

Based on the promising results of the AuDAC sample, gold nanoparticles were also prepared using DAAL, DAH, and DADXA. The synthesis were same as for AuDAC and reaction parameters were chosen based on the studies previously performed for AuDAC. After forming AuNPs, characterized by the pink coloration, the samples were cooled in a water bath in a refrigerator, followed by acid dialysis in demineralized water at pH 3.5. For the AuDAH and AuDADXA, the reaction was instantaneous. The AuDAAL sample did not change color immediately, so it was left to react in the oil bath for 20 min after adding reagents.

6.1.3 Preparation of composite material from AuDAC and chitosan nanofibers

Chitosan nanofibers were prepared by electrospinning from a chitosan solution dissolved in acetic acid and with PEO at CPS in collaboration with Dr. Kimmer's group. The nanofibers were spun onto a polypropylene substrate and cut into squares. The chitosan nanofibers prepared in this way were subsequently used for the screening study of so-called affinity anchoring of AuDAC nanoparticles, see below in section 7.4. In the experiment, one-quarter of the prepared chitosan nanofiber squares have been used. These were subsequently immersed in AuDAC solution in which the pH was adjusted to 7 after acid dialysis to prevent chitosan dissolution. The affinity anchoring reaction ran over a time range of 1 to 168 h. After the set time had elapsed, the squares were washed in demineralized water and then placed in STAB (Sodium triacetoxyborohydride) solution containing twice the molar excess to the number of -CHO groups contained in a given amount of DAC used. This process stabilized the bond between the chitosan nanofibers and the gold nanoparticles. The samples were then rewashed in demineralized water, lyophilized, and characterized by available methods.

Based on this study, a bulk composite material was created by mixing chitosan nanofibers with AuDAC solution using a mechanical homogenizer and incubating shaker. Binding was carried out for 3 h according to the results from the study, after which the sample was filtered and centrifuged. The reduction of the imine-

to-amine bond was then performed using a STAB solution, and the material was again purified by dialysis and subsequently lyophilized. The bulk sample prepared this way was characterized and later used to assemble the catalytic device.

6.1.4 Preparation of composite mats from AuDAC, AuDAH, chitosan and PA nanofibers

Composite nanofiber mats were prepared by a slightly modified procedure described in the previous section. Chitosan nanofibers were prepared for the study using the same procedure as above in collaboration with Dr. Kimmer. The PA nanofibers were supplied already in fibre form by the same group. The nanofiber mats were given to be washed a day ahead in demineralized water. Subsequently, the PA and CHIT bodies were placed in solutions of AuDAC and AuDAH nanoparticles whose pH was adjusted to 6. Binding was carried out for 48 h for AuDAC and AuDAH on chitosan nanofibers, and 20 days for AuDAH on PA nanofibers to increase the binding efficiency. After binding, the specimens were placed in demineralized water, then in STAB solution (twice the molar excess of STAB to the number of -CHO groups contained in a given amount of polysaccharide), and again in demineralized water. Finally, the composite materials were dried at laboratory temperature when pressed. The binding efficiency of the AuNPs was determined for the specimens. In collaboration with prof. Humpolíček's group, antimicrobial tests were performed for *Staphylococcus aureus* CCM 4516 and *Escherichia coli* CCM 4517 bacterial strains according to EN ISO 20743 and ISO 22196 standards.

6.2 Characterization of samples

Samples were characterized by Fourier transform infrared spectrometry, ultraviolet–visible spectroscopy, dynamic light scattering, x-ray diffraction analysis, thermogravimetric analysis and transmission electron microscopy. A Raman microscope was used to investigate the effect of surface-enhanced Raman signal using AuNP solutions. For other methods and details, see the articles [70, 71].

6.3 Catalysis

The reduction of 4-NP to 4-AP using sodium borohydride was chosen to determine the catalytic activity of AuNP solutions because it allows a direct comparison with previous works [72]. The reduction was monitored as a decrease in absorbance at 400 nm, the wavelength at which 4-NP is manifested up to a constant absorbance value at the selected measurement temperature of 25 °C. The investigated solution consisted of 4-NP, NaBH₄, demineralized water, and AuNPs solution. For the individual ratios and concentrations of the substances, see previous works [70, 71]. A blank sample containing the corresponding amount of the polysaccharide solution in place of AuNPs was also measured.

The device shown in Figure 12 was used to determine the catalytic activity of the composite material. The thickness of the active catalytic layer was about 2 mm. The flow rate was set at 0.25, 0.5, and 0.75 mL/min. A medium that passed through the catalytically active layer was then analyzed on UV-Vis spectrometer. The experiments were repeated three times for each flow rate to determine reproducibility, and the equipment was washed with demineralized water between each test.

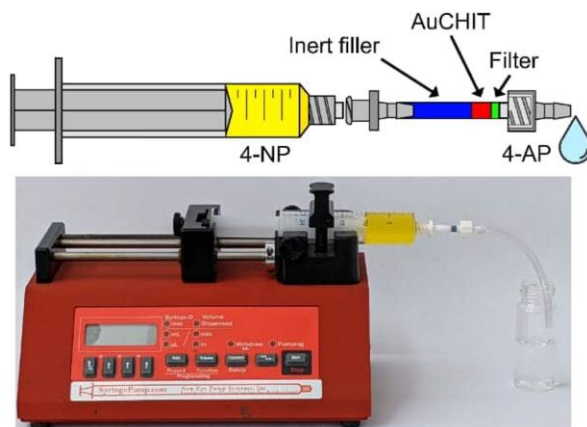


Figure 12: Scheme of the catalytic device [71]

7. RESULTS AND DISCUSSION

7.1 Preparation and characterization of polysaccharide derivatives

Different types of polysaccharides, namely dialdehyde cellulose (DAC), dialdehyde hyaluronan (DAH), dialdehyde dextran (DADXA), dialdehyde alginate (DAAL), dicarboxy hyaluronan (DCH), fully oxidized dicarboxy cellulose (DCC), and partially oxidized cellulose (DCC-70) with an oxidation degree of 70%, were prepared by selective oxidation. This process was confirmed by FT-IR spectrometry, see Figure 13. For the dicarboxy derivatives, the absorption band of the -C=O group vibration of -COOH appeared at 1600 cm^{-1} . This absorption band was also present for the DAH and DAAL samples because this group is primarily contained in the hyaluronic acid and alginate structure from which these derivatives are made. For DCH, there was only an increase in the intensity of this vibration, with oxidation tripling the number of its carboxyl groups. In addition, DAC, DAH, DAAL and DADXA showed characteristic absorption bands at 1735 cm^{-1} and 885 cm^{-1} , indicating carbonyl groups and hemiacetal structures, respectively.

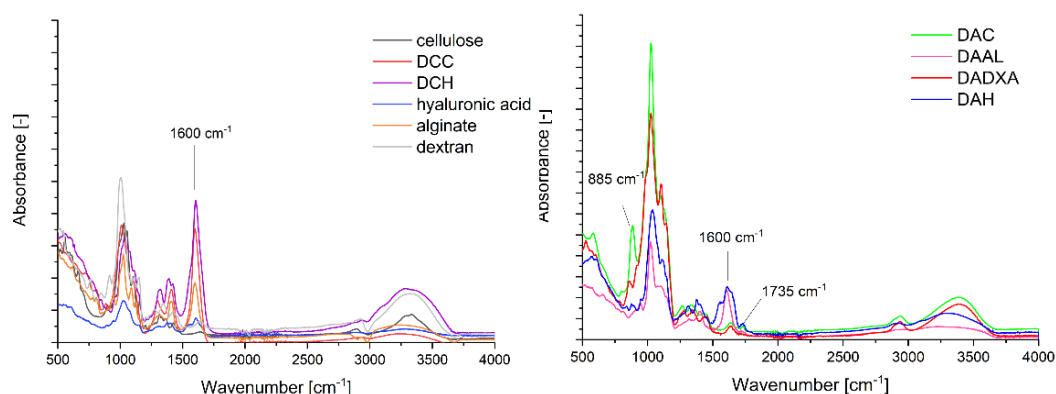


Figure 13: FT-IR spectra for cellulose, hyaluronic acid, dextran, alginate and DAC, DAH, DADXA, DAAL, DCC and DCH derivatives

Furthermore, DAC, DCC, DCC-70 and DCH were also characterized in terms of their changes in viscosity and structure. Table 1 shows their molecular weight distributions.

Table 1: Molecular weight of the prepared polysaccharides derivatives, M_w is weight-average molecular weight, M_n is number-average molecular weight, PDI is polydispersity index and DP is the degree of polymerization

	M_w [kDa]	M_n [kDa]	PDI [-]	DP [-]
DAC (converted to DCC)	14.0	8.5	1.65	53
DCC-70	2620/73.3	1688/40.4	1.5/1.8	12254/343

DCC	62.1	31.7	1.9	263
DCH	58.5	27.6	2.1	118

7.2 AuNPs from dicarboxy polysaccharides

AuNPs were first synthesized using the prepared and characterized dicarboxy polysaccharide derivatives: DCH, DCC, and DCC-70. For each material, optimization of reaction conditions, i.e. reaction time, polysaccharide concentration, and NaOH concentration in the reaction medium, was carried out. Available methods were then used to characterize AuNPs. Figure 14 shows an example of such optimization for the DCC derivative when the polysaccharide concentration was changed.

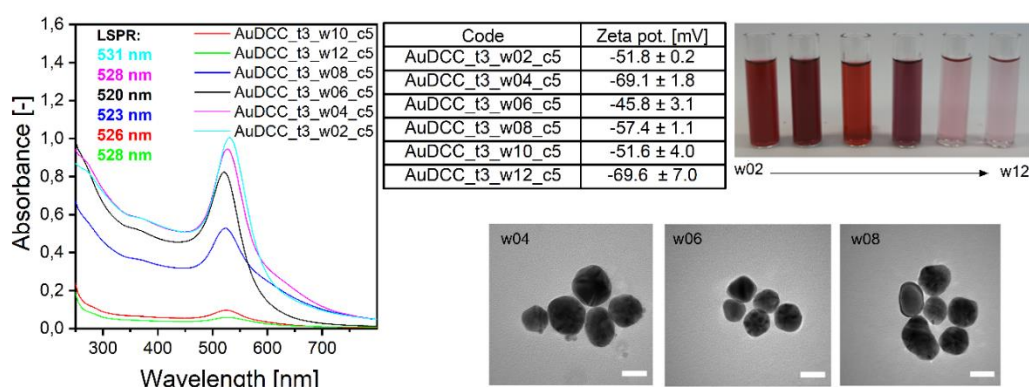


Figure 14: Screening study of gold nanoparticles prepared from fully oxidized DCC, UV-VIS spectrometry record, measured zeta potential values, TEM microscope images (white scale bar represents 20 nm) and macroscopic image of prepared solutions

The sample is always labeled with the type of polysaccharide derivative, synthesis time, polysaccharide weight content, and NaOH concentration. The parameters sought for the samples were the highest absorbance value with the lowest wavelength for the LSPR maximum. At the same time, however, they should be as stable as possible, i.e., the absolute value of the zeta potential should be greater than 30 mV. Furthermore, the homogeneity and shape of the prepared AuNPs were also evaluated by TEM analysis. See an article for more data on optimizing AuNP synthesis parameters [70].

Based on these studies, the most suitable parameters were selected for each AuNPs. For the gold nanoparticles prepared from DCC, it was a synthesis time of 3 h, a polysaccharide concentration of 0.6 wt. % and a NaOH concentration of 5 mmol/L, which gave rise to relatively homogeneous roughly spherical nanoparticles with a narrow size distribution of 21 ± 3 nm. These dimensions are due to the high reduction efficiency of DCC in combination with the highest density of -COOH groups. AuDCCs also had the highest shell-to-core ratio among all samples, containing only 19% gold core and 81% DCC, which corresponds to

the derivative's high stabilization potential caused by the highest density of COOH groups.

For AuDCC-70, the final synthesis time was 3 h, the polysaccharide concentration was 0.4 wt.% and the NaOH concentration was 5 mmol/L, which gave rise to particles of two different sizes - a larger one of about 30 nm in size and a smaller one of about 4 nm in size. The shell: core ratio for the AuDCC-70 sample was 58%: 42%, which is the lowest of all the nanoparticles and indicates that the DCC-70 derivative has the lowest stabilizing ability. On the contrary, however, due to their irregular shapes and the presence of nanoparticles below 10 nm, it seemed to be a suitable material for both catalytic activity and SERS amplification alike.

The most suitable parameters for AuDCH were set to a synthesis time of 5 h, a polysaccharide weight concentration of 0.4 wt.% and a NaOH concentration of 5 mmol/L, which gave rise to polyhedral nanoparticles with larger dimensions and a wider size distribution of 52 ± 13 nm corresponding to the weak reduction potential of the DCH derivative. With a core: shell ratio of 31%: 69%, it ranks between the two aforementioned samples indicating its medium stabilizing ability.

All samples were studied for stability as a function of pH and it was found that they all show good stability up to pH 12. On the contrary, with the increasing acidity of the environment, aggregation of nanoparticles occurred, especially below the pH value of 3. The AuDCC sample was the most stable at acidic pH, and the AuDCC-70 was the least stable, which corresponds to the thickness of their stabilization layer. Regarding temporal stability, the samples were remeasured after half a year of refrigerated storage, and the measured values of hydrodynamic radii and zeta potential were almost identical within the measurement error.

7.2.1 Reduction mechanism

A common mechanism for reducing gold salts by polysaccharides involves an equilibrium between the hemiacetal and aldehyde groups at the reducing end of the polysaccharide. While the aldehyde is oxidized to the carboxyl group and aldonic acid is formed, the Au^{III} salt is simultaneously reduced. For dicarboxy polysaccharides, however, the reduction mechanism is different, and its scheme, given in the example of DCC, is proposed in Figure 15. This is caused by the oxidation of reducing ends during the oxidation, leading to the formation of tartronate. Hence, tartronate hydrolysis has to occur first to expose a new reducing end of the polysaccharide derivative. The presence of tartronate was confirmed by NMR to support this mechanism. The newly formed DCC-reducing end can reduce gold salts according to a modified conventional procedure. The main difference is that instead of gluconic acid normally formed after hydrolysis of the hemiacetal bond, a small molecular aldehyde is released, which is then able to

reduce Au^{III} to Au⁰ while simultaneously converting to oxalate. The gold atoms then begin to form particle nuclei stabilized by the functional groups of the polysaccharide chain. This is followed by their growth to the final form of various sizes and shapes of gold nanoparticles. In the case of the DCH sample, the reducing ends can be formed by either oxidized glucuronic acid or N-acetyl-D-glucosamine. In the case of glucuronic acid, the reduction of gold salts would again involve a small molecular aldehyde. On the other hand, the N-acetyl-D-glucosamine-reducing ends will reduce the gold salts by a classical reduction mechanism.

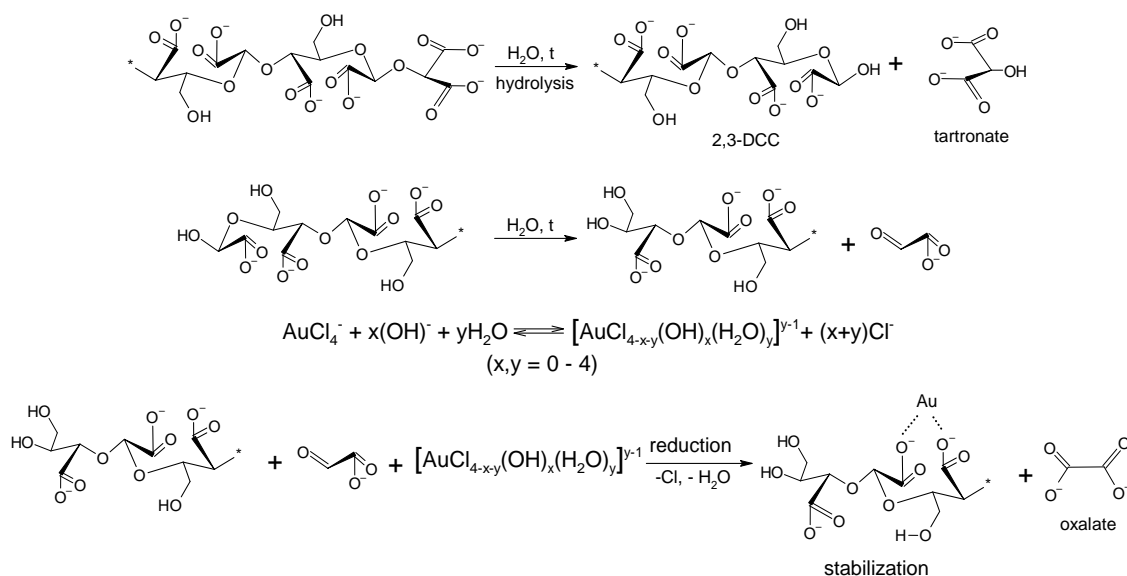


Figure 15: Scheme of Au salt reduction mechanism for DCC sample

7.2.2 SERS application

The prepared AuNP samples were shown to be able to enhance the Raman signal for the N-acetylcysteine (NAC) compound, as shown in Figure 16, while the signals of blank samples prepared only from pure NAC or AuNPs were below the detection limit. However, when comparing the spectra of surface-enhanced NAC using AuNPs and conventional powdered NAC, it can be seen that the bands shifted slightly towards higher wavenumbers. This effect may be due to the formation of weak interactions between NAC and the surface of AuNPs during adsorption. The AuDCH sample is the most promising for the SERS effect, which is logical given that it has the most irregular nanoparticle shapes of all prepared AuNPs, which are crucial for the SERS effect. On the contrary, the slightest enhancement was observed for the AuDCC sample, composed of small homogeneous spherical nanoparticles.

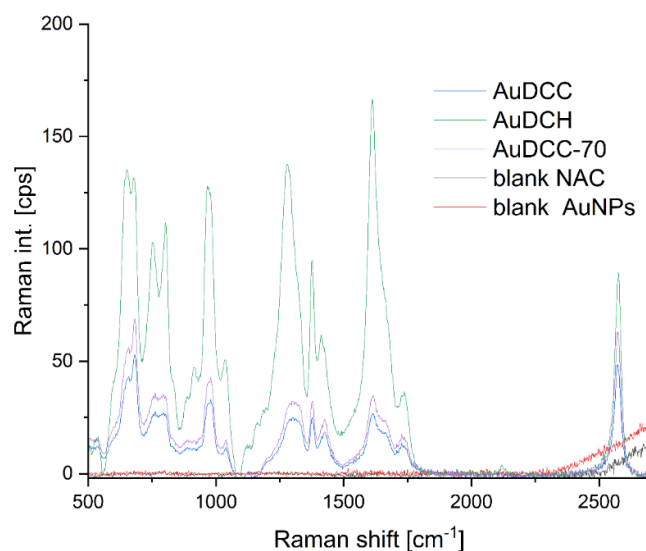


Figure 16: Comparison of SERS effect on NAC compound signal using AuDCC, AuDCC-70 and AuDCH samples

7.2.3 Catalytic activity

The catalytic activity of the prepared AuNPs samples was demonstrated by the reduction of 4-NP to 4-AP, which proceeds according to the scheme see Figure 2. The decrease in absorbance was monitored at 400 nm, which is the characteristic wavelength for 4-NP, the concentration of which decreased during the reaction. A blank measurement was also performed where the corresponding amount of the polysaccharide derivative replaced the AuNP sample. As seen from the Figure 17 left diagram, no reduction occurs in this case. The reduction reaction of 4-NP exhibits first-order pseudo kinetics, evident from the linear dependence of $\ln(c/c_0)$ on the reaction time (see Figure 17 right graph). From this dependence, the reaction rate constants (k) were calculated and the turnover frequency (TOF) was subsequently derived. TOF corresponds to the moles of reactant converted to the molar amount of catalyst per minute and was calculated relative to the initial concentration of 4-NP, according to the literature [73]. The results were compared with publications dealing with AuNP systems with polysaccharides, see article [70]. Due to its composition, the AuDCC sample, which consists of small homogeneous spherical particles, was the most suitable for catalysis. On the other hand, AuDCH was the least suitable for catalysis because of its larger particles, i.e. large and irregular particles.

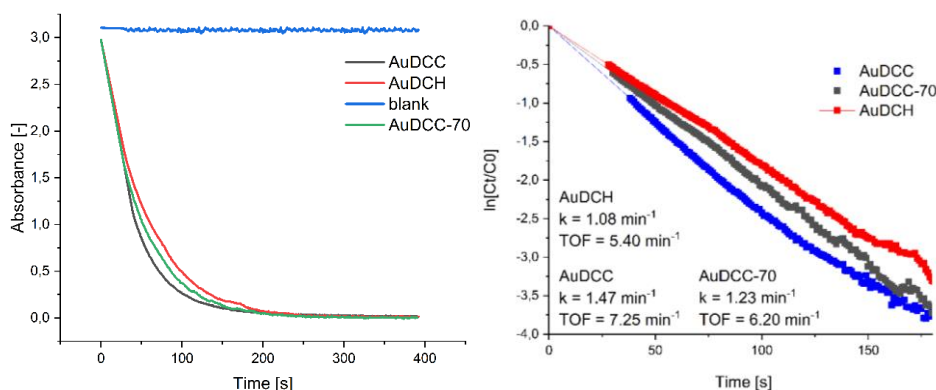


Figure 17: Catalytic activity of AuNPs investigated for the reduction of 4-NP to 4-AP. On the left, dependence of the decrease in absorbance with time, investigated at a wavelength of 400 nm characteristic of 4-NP. On the right, dependence of $\ln(c/c_0)$ on reaction time, calculated value of k and TOF

7.3 Screening study of AuNPs from dialdehyde cellulose

Cellulose dialdehyde was used to prepare AuNPs, and the optimization of the synthesis parameters, namely, the weight concentration of DAC, the concentration of gold precursor, and the concentration of NaOH, was carried out. The resulting nanoparticle solutions were investigated based on the wavelength and LSPR values, their stability, morphology, and size distribution. The parameters were optimized to achieve AuDAC of the smallest size with the greatest stability. An example of one of these studies where the most suitable DAC weight concentration was determined is shown in Figure 18.

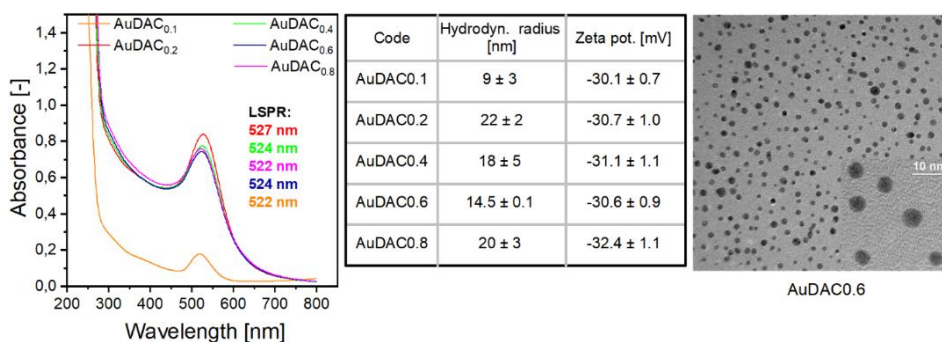


Figure 18: Screening study of AuDAC with different DAC weight concentration, UV-VIS spectrometry record, measured zeta potential and hydrodynamic radius values and TEM microscope images of AuDAC06 sample

Based on screening, see article [71], 0.6 wt. % DAC, 0.5 mg/mL HAuCl₄·3H₂O and 200 µg/mL NaOH appear to be the most suitable parameters for preparing AuDAC, as they give rise to homogeneous spherical nanoparticles of approximately 5 nm in size. Thus, both the reduction and stabilization capacity of the DAC was confirmed. For the DAC derivative, the aldehyde groups are oxidized to carboxyl groups during the reduction of the Au^{III} complex, and the

AuNPs are then electrostatically stabilized. Moreover, it was found that the synthesis is several times faster than syntheses using native polysaccharides or their dicarboxy derivatives.

7.4 AuDAC and chitosan nanofiber composite

This composite was prepared using the so-called affinity anchoring method. The excess of carbonyl groups in the shell of the prepared AuDAC solutions were used to react with the amine groups contained in the chitosan nanofibers to form the composite material. Since the imine bonds formed through the Schiff base reaction are reversible and hence prone to disruption in an acidic environment, imine bond reduction by STAB was employed, cf Figure 9 again. Formation of stable secondary amine bond increased the stability of the AuDAC/chitosan composite. The time dependence of the anchoring reaction of AuDAC solution on chitosan nanofibers was also studied from 1 to 168 h. In particular, the residual LSPR intensity of AuDAC solutions was monitored by UV-VIS analysis, supplemented by SEM and TEM recordings. Based on the study, 3 h of loading was optimal because the nanofiber coverage was sufficient in the shortest possible time. In addition, as can be seen in Figure 19, after 168 h, the surface of the composite started to disintegrate, and AuCHIT clusters began to form in the solution.

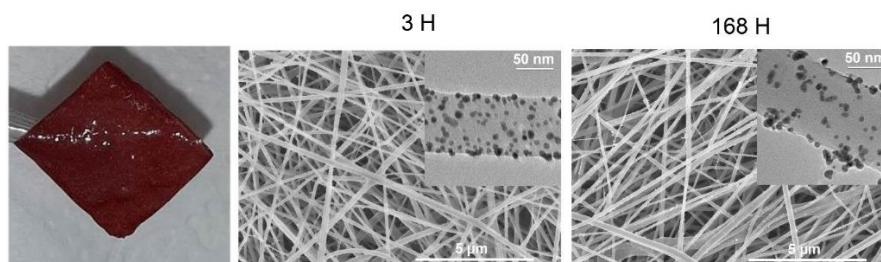


Figure 19: Image of AuCHIT composite and TEM and SEM images of 3 and 168 h AuCHIT time series samples

Based on this study, the final composite sample was prepared. A mechanical homogenizer was used to increase the surface area of nanofibers available for affinity anchoring of AuNPs, thereby increasing the efficiency of the given process. UV-Vis and XRF analysis later confirmed the effective binding of AuNPs, see article [71]. The absorption band of the original AuDAC solution at a wavelength of 524 nm completely disappeared after 3 h of reaction with homogenized nanofibers. At the same time, the XRF value of the remaining AuDAC solution after 3 h of binding was determined to be 0.0021 mg/mL Au, which means that about 99% of gold nanoparticles were bound to the chitosan nanofibers. The stability of the resulting composite exposed to PBS solutions of pH 3, 7, and 9 for 24 h was also checked. According to the SEM and TEM images, see Figure 20, it is evident that there were no changes in the structure of both nanofibers and AuDAC.

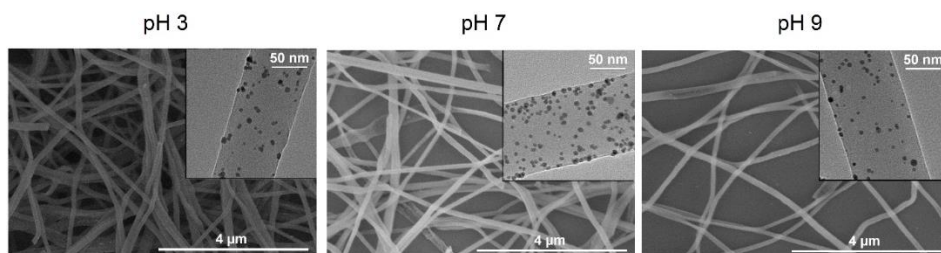


Figure 20: Stability of the final composite material in a PBS solution of pH 3, 7 and 9.

7.4.1 The catalytic activity of AuDAC and composite material

As in the previous case, the catalytic activity of the AuDAC sample and the AuCHIT composite was investigated on the reduction of 4-NP to 4-AP in the presence of sodium borohydride. Thus, the decrease in the concentration of the 4-NP compound at 400 nm as a function of reaction time was again monitored for AuDAC. Furthermore, the dependence of $\ln(c/c_0)$ on reaction time was plotted, and the rate constant k and TOF values were determined. This was done for two AuDAC solutions of different concentrations, as shown in the left graph in Figure 21. Using 2 μg AuDAC, 90% of 4-NP was reduced to 4-AP within 7 min, indicating a significant increase in catalytic efficiency compared to previous AuNP samples prepared from dicarboxy derivatives of the polysaccharides. Since the AuDAC sample contains the smallest nanoparticles among all the AuNP samples prepared so far, it is logical that it provided the best catalytic efficiency. If we reduce the AuDAC concentration ten times, the TOF value increases by a factor of two and the rate constant decreases by a factor of four, i.e. the TOF value was 27.1 min^{-1} , and the rate constant was 0.07 min^{-1} .

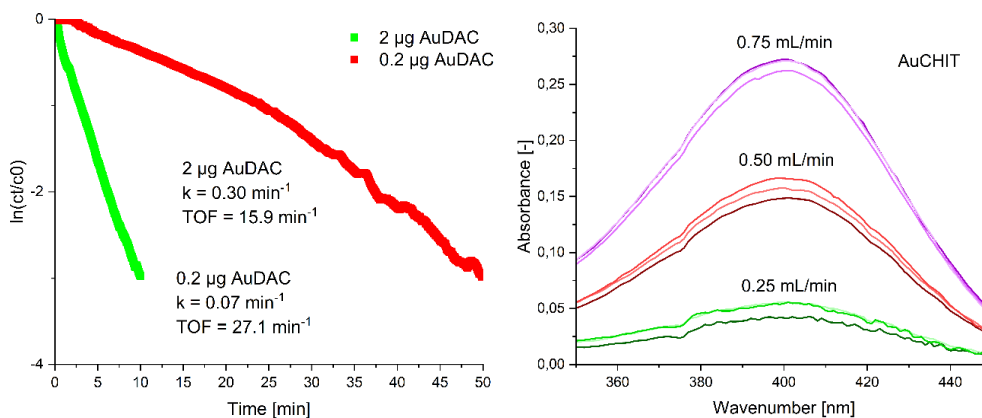


Figure 21: Catalytic activity of AuDAC sample and composite AuCHIT material from AuDAC and chitosan nanofibers

The catalytic efficiency of the AuCHIT composite material cannot be studied directly due to its insolubility, which could affect the UV-Vis measurements. Therefore, a catalytic device was assembled for the given experiment, see Figure 12, where the flow of the medium determines the catalytic efficiency. Records of individual flow rates, when the experiment was repeated 3 times for each, are

shown in Figure 21 on the right graph. At the fastest flow rate, i.e. 0.75 mL/min, 4-NP was reduced to 4-AP by approximately 92 %. Slower flow rates then showed an even more effective reduction, with a conversion of almost 99 % at 0.25 mL/min. From the linear dependence of 4-NP on 4-AP, it can be concluded that 90% conversion corresponds to a flow rate of 1 mL/min. TOF parameter for a rate of 0.75 mL/min was 0.28 min^{-1} . Although smaller than for free AuNPs, the reduction took place quickly due to the thickness of the active catalytic layer of approximately 2 mm, which corresponds to a reaction time of only several seconds at a given flow. In addition, catalytic efficiency was slightly increased during cycle repetitions for individual flow rates. This phenomenon can be explained by the partial swelling of the active layer of the composite material with an increasing number of cycles.

7.5 Catalytic activity of AuDAH, AuDAAL and AuDADXA

Based on the promising results of the AuDAC sample, gold nanoparticles were prepared using other dialdehyde derivatives of polysaccharides, namely DAAL, DAH and DADXA. The resulting AuNPs were characterized by UV-Vis spectrometry, see the left side of Figure 22. From the record and the observed LSPR values, it is evident that the smallest nanoparticles were prepared using dialdehyde dextran with a relatively homogeneous distribution, followed by AuDAAL sample. On the other hand, the AuDAH sample consisted of larger particles with a wide distribution, which was already evident from the purple colouration of the solution, compared to the other two, which were red. DLS measurement subsequently confirmed these results, where the hydrodynamic radius and polydispersity index of individual AuNPs were determined, see right side of Figure 22.

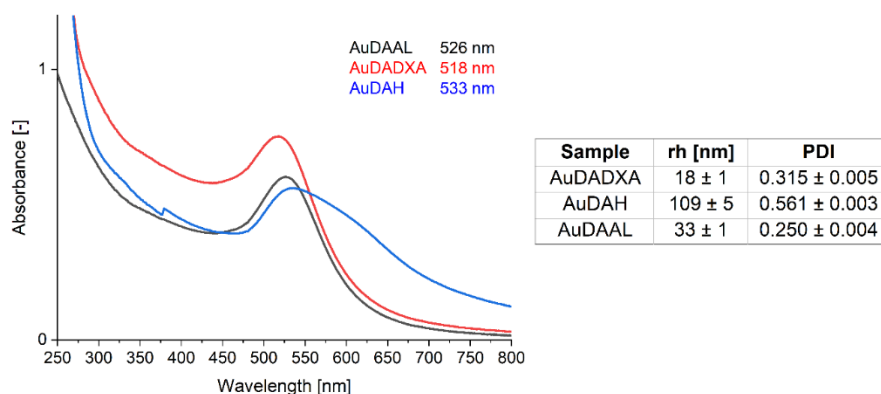


Figure 22: UV-Vis spectra with LSPR values for AuDAAL, AuDADXA and AuDAH and their hydrodynamic radius (r_h) values with a polydispersity index (PDI)

The catalytic activity for reducing 4-NP was subsequently measured on the samples. Again, the time dependence of the basic logarithm of the ratio of the 4-NP concentration over time to the 4-NP concentration at the beginning of the reaction was plotted on a graph, and the k and TOF values were calculated, see

Figure 23. According to the results, the AuDADXA with a rate constant of 0.78 min^{-1} and a TOF of 37.1 min^{-1} is the most efficient for this application, which is consistent with the fact that it was the sample with the smallest particles and, therefore, the largest nanoparticle surface area to allow catalytic reduction. The catalytic activity decreased with increasing nanoparticle size and was the slowest for the AuDAH. Nevertheless, compared to the AuDAC sample from the previous study, the catalytic reductions using AuDAAL, AuDAH and AuDADXA were more efficient.

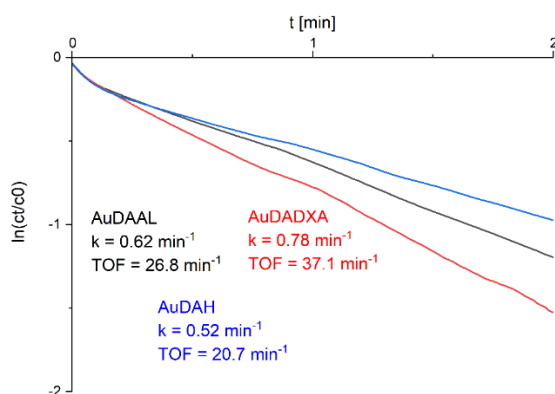


Figure 23: Dependence of $\ln(c/c_0)$ on reaction time, calculated values of k and TOF of AuDAAL, AuDADXA and AuDAH for catalytic reduction of 4-NP

7.6 Composite materials from AuDAC, AuDAH, chitosan and PA nanofibers

Successful anchoring of AuDAC nanoparticles to chitosan nanofibers was achieved using Schiff base formation between the excess carbonyl groups in the AuNP shell and the amine groups contained in the chitosan nanofibers. In the subsequent study, the AuDAC nanoparticles are bonded to polyamide nanofibers, which also have amine groups in their structure. The choice of binding time was set to 48 h due to the slower binding to PA nanofibers. Anchoring of another type of nanoparticles, namely AuDAH, was also tested and the coupling time to PA nanofibers was extended up to 20 days to increase the efficiency, see Figure 24. Using DLS analysis, the hydrodynamic radii of nanoparticles in the starting solutions were found to be $33.6 \pm 0.6 \text{ nm}$ with a PDI of 0.46 ± 0.03 for AuDAC and $25.6 \pm 0.5 \text{ nm}$ with a PDI of 0.39 ± 0.02 for AuDAH. The amount of gold bound per mg of filament body was calculated based on the masses of the filament bodies and the gold concentrations determined by X-ray fluorescence analysis from the solutions before and after binding. This quantity is influenced not only by the binding time but also by the number of carbonyl and amine groups available for Schiff base formation. Since a sample of PA fibers weighed on average three times less than a square of chitosan fibers and had less amine groups, less gold was also bound to it, which is also evident from the intensity of the coloration of the individual bodies.

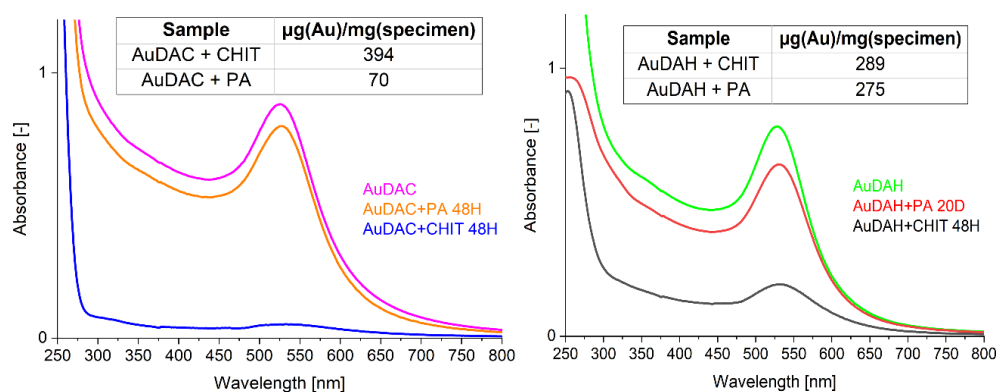


Figure 24: UV-Vis spectra of starting solutions of AuDAC and AuDAH and spectra of solutions after binding to polyamide and chitosan nanofibers with the amount of AuNPs attached to fibre bodies

The antibacterial activity for the bacterial strains *Staphylococcus aureus* CCM 4516 and *Escherichia coli* CCM 4517 was subsequently performed on the prepared bodies in collaboration with Prof. Humpolíček's group. The activity for pure nanofibers was also included in the results as a blank. Table 2 shows the activity values for each sample, where the effectiveness of antibacterial properties is evaluated by number A. If A is less than 2, the antibacterial efficacy is low; if A takes values between 2 and 3, the effectiveness is significant, and if the values are higher than 3; the antibacterial activity is strong. Most samples showed low antibacterial activity against both strains. The exception was the AuDAC sample on chitosan nanofibers, which showed strong antibacterial activity for the gram-positive bacteria *Staphylococcus aureus* CCM 4516. However, it must be taken into account that this study is still ongoing and that further measurements need to be completed, such as testing the cytotoxicity of the given materials or confirmation of the density of coverage of the composite bodies with gold nanoparticles using TEM microscopy.

Table 2: Antibacterial activity for composite samples for bacterial strains *Staphylococcus aureus* CCM 4516 and *Escherichia coli* CCM 4517

Sample	<i>Staphylococcus aureus</i>	<i>Escherichia coli</i>
	A [-]	A [-]
AuDAC + CHIT	5.145	1.484
AuDAH + CHIT	1.520	1.296
AuDAC + PA	1.324	0.676
AuDAH + PA	0.240	0.347

CONCLUSIONS

The literature review showed the usefulness and application potential of the gold nanoparticles as well as the structural and functional suitability of modified biopolymers to synthesize gold nanoparticles and construct composite materials with functionalities imparted by the gold nanoparticle incorporation. Although polysaccharides are commonly used for Au salt reduction to obtain gold nanoparticles, the control over the result is often limited. Based on thoroughly considering the state-of-the-art, available experience and original ideas, the dissertation work was conceived to extend the knowledge beyond the contemporary limits. The work aimed to study the preparation and properties of AuNPs prepared using selectively oxidized polysaccharides of different types and degrees of oxidation, including tailoring a composite material incorporating prepared nanoparticles for catalytic function.

The initial hypothesis was confirmed that dicarboxypolysaccharides, despite state-of-the-art expectations, can reduce gold salts to gold nanoparticles, yielding products with suitable size distribution and shape characteristics for eventual utilization in catalytic activity and spectroscopic analysis employing the Surface-Enhanced Raman Scattering (SERS) effect. Selectively dicarboxylated cellulose (DCC) and hyaluronate (DCH) were successfully used as reducing and capping agents for gold nanoparticles (AuNPs) synthesis, and the reaction mechanism was explained. Whereas partially oxidized polysaccharides containing available aldehyde groups can reduce Au^{III} complexes via the classic reduction mechanism, the fully oxidized DCPs should be – at least in theory – non-reducing polysaccharides. Nevertheless, it was discovered that first tartronate hydrolysis at the end of the DCP chain has to occur to expose a new reaction centre together with the release of a small aldehyde molecule (tartronate), which is then able to reduce Au^{III} to Au⁰ while simultaneously converting to oxalate.

It was demonstrated that the structure of the dicarboxypolysaccharides affects the size of the nanoparticles, and the examined modified polysaccharides can stabilize AuNPs against aggregation. Using fully-oxidized DCC with the homogenous structure and high density of carboxyl groups in gold source compound reduction induces isotropic growth of nanoparticles, resulting in the smallest and most stable uniform AuNPs with good catalytic performance in 4-nitrophenol (4-NP) to 4-aminophenol (4-AP) reduction. Examining the other DCPs, it was confirmed that the catalytic activity of AuNPs diminishes with increasing particle size.

Another interesting feature of gold nanoparticles is that they can enhance SERS effect. Dicarboxylated hyaluronate induced anisotropic growth of larger polyhedral and irregular AuNPs ($d \sim 50$ nm nanoparticles) due to its lower stabilizing potential and slower reduction rates. Obtained nanoparticles exhibited 9 times stronger Raman signals on average compared to AuNPs obtained using

DCC. It was also demonstrated that AuNPs with uneven shapes and irregular surfaces provide increased Surface-Enhanced Raman Scattering efficacy.

There is a trade-off between maximum catalytic efficiency experienced for the smallest nanoparticles and the strength of the SERS signals observed for large and irregular nanoparticles. As a result, selectively dicarboxylated cellulose (DCC) and hyaluronate (DCH) prepared by controlled oxidative modification can be used as reducing and capping agents for AuNPs synthesis, allowing for the preparation of nanoparticles optimized towards catalytic or SERS function. Thus, the way the composition and properties of the modified polysaccharides can be intentionally adjusted for desired AuNPs tailoring was discovered.

The second part of the dissertation delved into utilizing the oxidized polysaccharides as reducing and stabilizing agents and as macromolecular support in synthesizing gold nanoparticles (AuNPs). In contrast to traditional approaches in nanotechnology like spin coating or dip coating, where AuNPs are generally bound to the support or substrate only by weak interactions, a two-stage approach for preparing composites with covalently anchored AuNPs on chitosan substrate was proposed.

First, 5 nm AuNPs with high catalytic activity were synthesized and stabilized using dialdehyde cellulose (DAC) via the classic reduction mechanism. Next, the stabilizing shell of the nanoparticles was further used to attach the nanoparticles to the chitosan substrate as the reduction capacity of DAC was not fully depleted in Au^{III} to Au⁰ reduction. The aldehyde groups remaining in the shell of prepared nanoparticles were used to tether AuNPs to chitosan nanofibers with quantitative efficacy in a process for which the term “affinity anchoring” is coined. Schiff bases formed during this process were subsequently reduced to secondary amines by borohydride, significantly improving the gold-chitosan nanocomposite (AuCHIT) stability in the broad pH range from 3 to 9.

The catalytic efficacy of the resulting composite was demonstrated using a model catalytic device representing an industrial catalytic column, thus providing more realistic results. Reduction of 4-NP to 4-AP in the presence of borohydride was again used for testing the AuCHIT performance. The material showed high stability and fast conversion rates.

To generalize, the modification potential of AuNPs stabilized by a reactive DAC shell, and especially their affinity towards amines, open up new possibilities beyond the catalysis field, particularly in biomedical applications such as the development of therapeutic agents, biosensors, or attachment of targeting vectors for drug delivery. Future research may also explore different kinds of metal nanoparticles that could be prepared using this approach and “affinity anchored” to any substrates containing amine or even amide groups, going far beyond the scope of described results and further expanding the ideas proposed in the thesis.

CONTRIBUTION TO SCIENCE AND PRAXIS

The contributions of this work to science and general practice include demonstrating the ability of selectively oxidized derivatives, namely hyaluronic acid, dextran, alginate, and cellulose derivatives, to reduce gold salt complexes and stabilize the resulting gold nanoparticles. In addition, a modified reduction mechanism was proposed for dicarboxy polysaccharides because the process differs from the conventional mechanism for reducing gold salts by polysaccharides.

The effects of individual synthesis parameters on the sizes and shapes of the resulting nanoparticles were also determined. Subsequently, the application potential of the gold nanoparticles was demonstrated, specifically for the catalytic application and the Surface-Enhanced Raman Scattering effect. The gold nanoparticles with the smallest possible size prepared using dialdehyde dextran were the most suitable for the catalytic reduction of 4-nitrophenol to 4-aminophenol. In contrast, relatively large nanoparticles with irregular shapes prepared using dicarboxy hyaluronic acid were the best for the Surface-Enhanced Raman Scattering effect.

Furthermore, the affinity anchoring of gold nanoparticles prepared using dialdehyde cellulose to chitosan nanofibers via Schiff base formation between the amine group of chitosan and the carbonyl group of gold nanoparticles was also demonstrated. Moreover, the catalytic efficiency of this composite material was shown on an original assembled device modelling the reaction column. It was also confirmed that this anchoring method could be used for different types of gold nanoparticles prepared using different polysaccharide derivatives, and attached to various nanofibres containing amine groups. In the very last study, the antibacterial activity of most of the materials was low, but gold nanoparticles prepared using dialdehyde cellulose anchored on chitosan nanofibers showed strong efficacy against gram-positive bacteria *Staphylococcus aureus*.

The aforementioned contributions do not only represent scientific achievements but also open a way for the application of these material designs in further study and development of (i) biomedical materials and devices for wound healing, especially efficient towards nosocomial infections, (ii) analytical applications of SERS, (iii) applications in catalysis, and many others.

REFERENCES

- [1] POOJA, Deep, Sravani PANYARAM, Hitesh KULHARI, Bharathi REDDY, Shyam S. RACHAMALLA a Ramakrishna SISTLA. Natural polysaccharide functionalized gold nanoparticles as biocompatible drug delivery carrier. *International Journal of Biological Macromolecules* [online]. 2015, **80**, 48–56. ISSN 0141-8130. Available from: doi:10.1016/j.ijbiomac.2015.06.022
- [2] CAO, Guozhong. *Nanostructures and Nanomaterials: Synthesis, Properties and Applications* [online]. B.m.: PUBLISHED BY IMPERIAL COLLEGE PRESS AND DISTRIBUTED BY WORLD SCIENTIFIC PUBLISHING CO., 2004 [vid. 2023-01-22]. ISBN 978-1-86094-415-4. Available from: doi:10.1142/p305
- [3] PANDEY, Sadanand, Gopal K. GOSWAMI a Karuna K. NANDA. Green synthesis of polysaccharide/gold nanoparticle nanocomposite: An efficient ammonia sensor. *Carbohydrate Polymers* [online]. 2013, **94**(1), 229–234. ISSN 0144-8617. Available from: doi:10.1016/j.carbpol.2013.01.009
- [4] UTHAMAN, Saji, Hyeon Sik KIM, Vishnu REVURI, Jung-Joon MIN, Yong-kyu LEE, Kang Moo HUH a In-Kyu PARK. Green synthesis of bioactive polysaccharide-capped gold nanoparticles for lymph node CT imaging. *Carbohydrate Polymers* [online]. 2018, **181**, 27–33. ISSN 0144-8617. Available from: doi:10.1016/j.carbpol.2017.10.042
- [5] MÜNSTER, Lukáš, Michaela FOJTŮ, Zdenka CAPÁKOVÁ, Tomáš VACULOVÍČ, Michaela TVRDOŇOVÁ, Ivo KUŘITKA, Michal MASÁŘÍK a Jan VÍCHA. Selectively Oxidized Cellulose with Adjustable Molecular Weight for Controlled Release of Platinum Anticancer Drugs. *Biomacromolecules* [online]. 2019, **20**(4), 1623–1634. ISSN 1526-4602. Available from: doi:10.1021/acs.biomac.8b01807
- [6] MÜNSTER, L., B. HANULÍKOVÁ, M. MACHOVSKÝ, F. LATEČKA, I. KUŘITKA a J. VÍCHA. Mechanism of sulfonation-induced chain scission of selectively oxidized polysaccharides. *Carbohydrate Polymers* [online]. 2020, **229**, 115503. ISSN 1879-1344. Available from: doi:10.1016/j.carbpol.2019.115503
- [7] MUNSTER, Lukas, Michaela FOJTU, Zdenka CAPAKOVA, Monika MUCHOVA, Lenka MUSILOVA, Tomas VACULOVIC, Jan BALVAN, Ivo KURITKA, Michal MASARIK a Jan VICHA. Oxidized polysaccharides for anticancer-drug delivery: What is the role of structure? *Carbohydrate Polymers* [online]. 2021, **257**, 117562. ISSN 0144-8617. Available from: doi:10.1016/j.carbpol.2020.117562

- [8] YANG, Jisheng, Suyu HAN, Haicheng ZHENG, Hongbiao DONG a Jiubing LIU. Preparation and application of micro/nanoparticles based on natural polysaccharides. *Carbohydrate Polymers* [online]. 2015, **123**, 53–66. ISSN 0144-8617. Available from: doi:10.1016/j.carbpol.2015.01.029
- [9] LEE, Byung Kook, Yeon Hee YUN a Kinam PARK. Smart Nanoparticles for Drug Delivery: Boundaries and Opportunities. *Chemical engineering science* [online]. 2015, **125**, 158–164. ISSN 0009-2509. Available from: doi:10.1016/j.ces.2014.06.042
- [10] BHATIA, Saurabh. Nanoparticles Types, Classification, Characterization, Fabrication Methods and Drug Delivery Applications. In: Saurabh BHATIA, ed. *Natural Polymer Drug Delivery Systems: Nanoparticles, Plants, and Algae* [online]. Cham: Springer International Publishing, 2016 [vid. 2023-04-18], s. 33–93. ISBN 978-3-319-41129-3. Available from: doi:10.1007/978-3-319-41129-3_2
- [11] GILJOHANN, David A., Dwight S. SEFEROS, Weston L. DANIEL, Matthew D. MASSICH, Pinal C. PATEL a Chad A. MIRKIN. Gold Nanoparticles for Biology and Medicine. *Angewandte Chemie International Edition* [online]. 2010, **49**(19), 3280–3294. ISSN 1521-3773. Available from: doi:10.1002/anie.200904359
- [12] DREADEN, Erik C., Alaaldin M. ALKILANY, Xiaohua HUANG, Catherine J. MURPHY a Mostafa A. EL-SAYED. The golden age: gold nanoparticles for biomedicine. *Chemical Society Reviews* [online]. 2012, **41**(7), 2740–2779. ISSN 1460-4744. Available from: doi:10.1039/C1CS15237H
- [13] JENKINS, Julie A., Terianna J. WAX a Jing ZHAO. Seed-Mediated Synthesis of Gold Nanoparticles of Controlled Sizes To Demonstrate the Impact of Size on Optical Properties. *Journal of Chemical Education* [online]. 2017, **94**(8), 1090–1093. ISSN 0021-9584. Available from: doi:10.1021/acs.jchemed.6b00941
- [14] BALAMURUGAN, B. a Toshiro MARUYAMA. Evidence of an enhanced interband absorption in Au nanoparticles: Size-dependent electronic structure and optical properties. *Applied Physics Letters* [online]. 2005, **87**(14), 143105. ISSN 0003-6951. Available from: doi:10.1063/1.2077834
- [15] PETER N. NJOKI, I-IM S. LIM, DERRICK MOTT, † HYE-YOUNG PARK, BILAL KHAN, SUPRAV MISHRA, RAVISHANKER SUJAKUMAR, and JIN LUO a Chuan-Jian ZHONG*. Size Correlation of Optical and Spectroscopic Properties for Gold Nanoparticles. *ACS*

Publications [online]. 18. září 2007 [vid. 2023-04-19]. Available from: doi:10.1021/jp074902z

- [16] KHLEBTSOV, Boris N., Roman S. TUMSKIY, Andrey M. BUROV, Timofey E. PYLAEV a Nikolai G. KHLEBTSOV. Quantifying the Numbers of Gold Nanoparticles in the Test Zone of Lateral Flow Immunoassay Strips. *ACS Applied Nano Materials* [online]. 2019 [vid. 2023-04-19]. Available from: doi:10.1021/acsanm.9b00956
- [17] LIEBIG, Ferenc, Andreas F. THÜNEMANN a Joachim KOETZ. Ostwald Ripening Growth Mechanism of Gold Nanotriangles in Vesicular Template Phases. *Langmuir* [online]. 2016, **32**(42), 10928–10935. ISSN 0743-7463. Available from: doi:10.1021/acs.langmuir.6b02662
- [18] SINGH, Priyanka, Yeon Ju KIM, Chao WANG, Ramya MATHIYALAGAN a Deok Chun YANG. Microbial synthesis of Flower-shaped gold nanoparticles. *Artificial Cells, Nanomedicine, and Biotechnology* [online]. 2016, **44**(6), 1469–1474. ISSN 2169-1401. Available from: doi:10.3109/21691401.2015.1041640
- [19] MÂRZA, S. M., K. MAGYARI, S. BOGDAN, M. MOLDOVAN, C. PEȘTEAN, A. NAGY, F. TĂBĂRAN, E. LICARETE, S. SUARASAN, A. DREANCA, L. BAIA a I. PAPUC. Skin wound regeneration with bioactive glass-gold nanoparticles ointment. *Biomedical Materials* [online]. 2019, **14**(2), 025011. ISSN 1748-605X. Available from: doi:10.1088/1748-605X/aafd7d
- [20] OVAIS, Muhammad, Irshad AHMAD, Ali Talha KHALIL, Sudip MUKHERJEE, Rabia JAVED, Muhammad AYZAZ, Abida RAZA a Zabta Khan SHINWARI. Wound healing applications of biogenic colloidal silver and gold nanoparticles: recent trends and future prospects. *Applied Microbiology and Biotechnology* [online]. 2018, **102**(10), 4305–4318. ISSN 1432-0614. Available from: doi:10.1007/s00253-018-8939-z
- [21] MENAZEA, A. A. a M. K. AHMED. Wound healing activity of Chitosan/Polyvinyl Alcohol embedded by gold nanoparticles prepared by nanosecond laser ablation. *Journal of Molecular Structure* [online]. 2020, **1217**, 128401. ISSN 0022-2860. Available from: doi:10.1016/j.molstruc.2020.128401
- [22] HONG, Seongmin a Xiao LI. Optimal Size of Gold Nanoparticles for Surface-Enhanced Raman Spectroscopy under Different Conditions. *Journal of Nanomaterials* [online]. 2013, **2013**. Available from: doi:10.1155/2013/790323

- [23] HAO, Feng, Colleen L. NEHL, Jason H. HAFNER a Peter NORDLANDER. Plasmon Resonances of a Gold Nanostar. *Nano Letters* [online]. 2007, **7**(3), 729–732. ISSN 1530-6984. Available from: doi:10.1021/nl062969c
- [24] KUSTOV, L. M. Catalytic properties of supported gold nanoparticles in organic syntheses. *Russian Chemical Bulletin* [online]. 2013, **62**(4), 869–877. ISSN 1573-9171. Available from: doi:10.1007/s11172-013-0119-9
- [25] CORMA, Avelino a Hermenegildo GARCIA. Supported gold nanoparticles as catalysts for organic reactions. *Chemical Society Reviews* [online]. 2008, **37**(9), 2096–2126. ISSN 0306-0012. Available from: doi:10.1039/b707314n
- [26] HASHMI, A. Stephen K. Gold-Catalyzed Organic Reactions. *Chemical Reviews* [online]. 2007, **107**(7), 3180–3211. ISSN 0009-2665. Available from: doi:10.1021/cr000436x
- [27] ABBAS, Manzar, Hepi Hari SUSAPTO a Charlotte A. E. HAUSER. Synthesis and Organization of Gold-Peptide Nanoparticles for Catalytic Activities. *ACS Omega* [online]. 2022, **7**(2), 2082–2090. Available from: doi:10.1021/acsomega.1c05546
- [28] PAIDARI, Saeed a Salam Adnan IBRAHIM. Potential application of gold nanoparticles in food packaging: a mini review. *Gold Bulletin* [online]. 2021, **54**(1), 31–36. ISSN 2190-7579. Available from: doi:10.1007/s13404-021-00290-9
- [29] RASTOGI, Sarushi, Vinita KUMARI, Vasudha SHARMA a F. J. AHMAD. Gold Nanoparticle-based Sensors in Food Safety Applications. *Food Analytical Methods* [online]. 2022, **15**(2), 468–484. ISSN 1936-976X. Available from: doi:10.1007/s12161-021-02131-z
- [30] PHAN, Hoa T. a Amanda J. HAES. What Does Nanoparticle Stability Mean? *The Journal of Physical Chemistry C* [online]. 2019, **123**(27), 16495–16507. ISSN 1932-7447. Available from: doi:10.1021/acs.jpcc.9b00913
- [31] CORNIER, Jean, Cornelia M. KECK a Marcel VAN DE VOORDE, ed. *Nanocosmetics: From Ideas to Products* [online]. Cham: Springer International Publishing, 2019 [vid. 2023-10-31]. ISBN 978-3-030-16572-7. Available from: doi:10.1007/978-3-030-16573-4
- [32] XU, Liang, Hai-Wei LIANG, Yuan YANG a Shu-Hong YU. Stability and Reactivity: Positive and Negative Aspects for Nanoparticle Processing. *Chemical Reviews* [online]. 2018, **118**(7), 3209–3250. ISSN 0009-2665. Available from: doi:10.1021/acs.chemrev.7b00208

- [33] SCIMECA, Manuel, Simone BISCHETTI, Harpreet Kaur LAMSIRA, Rita BONFIGLIO a Elena BONANNO. Energy Dispersive X-ray (EDX) microanalysis: A powerful tool in biomedical research and diagnosis. *European journal of histochemistry: EJH* [online]. 2018, **62**(1), 2841. ISSN 2038-8306. Available from: doi:10.4081/ejh.2018.2841
- [34] ZHANG, Zhiheng, Yao HU, Hangyan JI, Qianzhu LIN, Xiaojing LI, Shangyuan SANG, David JULIAN MCCLEMENTS, Long CHEN, Jie LONG, Aiquan JIAO, Xueming XU, Zhengyu JIN a Chao QIU. Physicochemical stability, antioxidant activity, and antimicrobial activity of quercetin-loaded zein nanoparticles coated with dextrin-modified anionic polysaccharides. *Food Chemistry* [online]. 2023, **415**, 135736. ISSN 0308-8146. Available from: doi:10.1016/j.foodchem.2023.135736
- [35] MARTÍNEZ, Raquel, María F. NAVARRO POUPARD, Aitor ÁLVAREZ, Enrica SOPRANO, Martina MIGLIAVACCA, Carolina CARRILLO-CARRIÓN, Ester POLO, Beatriz PELAZ a Pablo del PINO. Chapter 2 - Nanoparticle behavior and stability in biological environments. In: Eun Ji CHUNG, Lorraine LEON a Carlos RINALDI, ed. *Nanoparticles for Biomedical Applications* [online]. B.m.: Elsevier, 2020 [vid. 2023-11-08], Micro and Nano Technologies, s. 5–18. ISBN 978-0-12-816662-8. Available from: doi:10.1016/B978-0-12-816662-8.00002-3
- [36] RAHMAN, Md Taifur a Evgeny V. REBROV. Microreactors for Gold Nanoparticles Synthesis: From Faraday to Flow. *Processes* [online]. 2014, **2**(2), 466–493. ISSN 2227-9717. Available from: doi:10.3390/pr2020466
- [37] ENUSTUN, B. V. a John. TURKEVICH. Coagulation of Colloidal Gold. *Journal of the American Chemical Society* [online]. 1963, **85**(21), 3317–3328. ISSN 0002-7863. Available from: doi:10.1021/ja00904a001
- [38] FRENS, G. Controlled Nucleation for the Regulation of the Particle Size in Monodisperse Gold Suspensions. *Nature Physical Science* [online]. 1973, **241**, 20–22. ISSN 0300-87460028-0836. Available from: doi:10.1038/physci241020a0
- [39] HUANG, Haizhen a Xiurong YANG. Synthesis of polysaccharide-stabilized gold and silver nanoparticles: a green method. *Carbohydrate Research* [online]. 2004, **339**(15), 2627–2631. ISSN 0008-6215. Available from: doi:10.1016/j.carres.2004.08.005
- [40] YUAN, Pengfei, Litong LIU, Adila AIPIRE, Yanan ZHAO, Shanshan CAI, Linjia WU, Xiaofei YANG, Alimu AIMAIER, Jun LU a Jinyao LI. Evaluation and mechanism of immune enhancement effects of *Pleurotus ferulae* polysaccharides-gold nanoparticles. *International Journal of*

- Biological Macromolecules* [online]. 2023, **227**, 1015–1026. ISSN 0141-8130. Available from: doi:10.1016/j.ijbiomac.2022.11.277
- [41] XU, Zhenbo. *Solubility of polysaccharides* [online]. 2018. ISBN 978-953-51-3650-7. Available from: doi:10.5772/66033
- [42] GOOSEN, Mattheus F. A. *Applications of Chitan and Chitosan*. B.m.: CRC Press, 1996. ISBN 978-1-56676-449-0.
- [43] SIRVIÖ, Juho Antti, Henrikki LIIMATAINEN, Jouko NIINIMÄKI a Osmo HORMI. Sustainable packaging materials based on wood cellulose. *RSC Advances* [online]. 2013, **3**(37), 16590–16596. ISSN 2046-2069. Available from: doi:10.1039/C3RA43264E
- [44] HEINZE, Thomas. Cellulose: Structure and Properties. In: Orlando J. ROJAS, ed. *Cellulose Chemistry and Properties: Fibers, Nanocelluloses and Advanced Materials* [online]. Cham: Springer International Publishing, 2016 [vid. 2023-04-10], *Advances in Polymer Science*, s. 1–52. ISBN 978-3-319-26015-0. Available from: doi:10.1007/12_2015_319
- [45] MARCHESSAULT, R. H. a P. R. SUNDARARAJAN. 2 - Cellulose. In: GERALD O. ASPINALL, ed. *The Polysaccharides* [online]. B.m.: Academic Press, 1983 [vid. 2023-04-07], s. 11–95. ISBN 978-0-12-065602-8. Available from: doi:10.1016/B978-0-12-065602-8.50007-8
- [46] PASCUAL (ALEJANDRO), Rodríguez a Eugenio Martín (E MARÍA). *Cellulose*. B.m.: BoD – Books on Demand, 2019. ISBN 978-1-83968-056-4.
- [47] ABATANGELO, G., V. VINDIGNI, G. AVRUSCIO, L. PANDIS a P. BRUN. Hyaluronic Acid: Redefining Its Role. *Cells* [online]. 2020, **9**(7), 1743. ISSN 2073-4409. Available from: doi:10.3390/cells9071743
- [48] PEREIRA, Hélder, Duarte Andre SOUSA, António CUNHA, Renato ANDRADE, J. ESPREGUEIRA-MENDES, J. Miguel OLIVEIRA a Rui L. REIS. Hyaluronic Acid. In: J. Miguel OLIVEIRA, Sandra PINA, Rui L. REIS a Julio SAN ROMAN, ed. *Osteochondral Tissue Engineering: Challenges, Current Strategies, and Technological Advances* [online]. Cham: Springer International Publishing, 2018 [vid. 2023-04-12], *Advances in Experimental Medicine and Biology*, s. 137–153. ISBN 978-3-319-76735-2. Available from: doi:10.1007/978-3-319-76735-2_6
- [49] SELYANIN, Mikhail A., Petr Ya BOYKOV, Vladimir N. KHABAROV a Felix POLYAK. *Hyaluronic Acid* [online]. B.m.: John Wiley & Sons, Ltd, 2015 [vid. 2023-04-12]. ISBN 978-1-118-63379-3. Available from: doi:10.1002/9781118695920

- [50] MOURYA, V. K. a Nazma N. INAMDAR. Chitosan-modifications and applications: Opportunities galore. *Reactive and Functional Polymers* [online]. 2008, **68**(6), 1013–1051. ISSN 1381-5148. Available from: doi:10.1016/j.reactfunctpolym.2008.03.002
- [51] DODANE, Valérie a Vinod D VILIVALAM. Pharmaceutical applications of chitosan. *Pharmaceutical Science & Technology Today* [online]. 1998, **1**(6), 246–253. ISSN 1461-5347. Available from: doi:10.1016/S1461-5347(98)00059-5
- [52] OGAWA, Kozo, Toshifumi YUI a Kenji OKUYAMA. Three D structures of chitosan. *International Journal of Biological Macromolecules* [online]. 2004, **34**(1), 1–8. ISSN 0141-8130. Available from: doi:10.1016/j.ijbiomac.2003.11.002
- [53] DÍAZ-MONTES, Elsa. Dextran: Sources, Structures, and Properties. *Polysaccharides* [online]. 2021, **2**(3), 554–565. ISSN 2673-4176. Available from: doi:10.3390/polysaccharides2030033
- [54] HEINZE, Thomas, Tim LIEBERT, Brigitte HEUBLEIN a Stephanie HORNIG. Functional Polymers Based on Dextran. In: Dieter KLEMM, ed. *Polysaccharides II* [online]. Berlin, Heidelberg: Springer, 2006 [vid. 2023-08-29], Advances in Polymer Science, s. 199–291. ISBN 978-3-540-37103-8. Available from: doi:10.1007/12_100
- [55] PLUCINSKI, Alexander, Zan LYU a Bernhard V. K. J. SCHMIDT. Polysaccharide nanoparticles: from fabrication to applications. *Journal of Materials Chemistry B* [online]. 2021, **9**(35), 7030–7062. Available from: doi:10.1039/D1TB00628B
- [56] ARAVAMUDHAN, Aja, Daisy RAMOS, Ahmed NADA a Sangamesh KUMBAR. Natural Polymers: Polysaccharides and Their Derivatives for Biomedical Applications. *Natural and Synthetic Biomedical Polymers* [online]. 2014, 67–89. ISSN 9780123969835. Available from: doi:10.1016/B978-0-12-396983-5.00004-1
- [57] ZHAO, Xihui, Zichao LI, Yujia DENG, Zhihui ZHAO, Xiaowen LI a Yanzhi XIA. Facile Synthesis of Gold Nanoparticles with Alginate and Its Catalytic Activity for Reduction of 4-Nitrophenol and H₂O₂ Detection. *Materials* [online]. 2017, **10**(5), 557. ISSN 1996-1944. Available from: doi:10.3390/ma10050557
- [58] CORMA, Avelino, Patricia CONCEPCIÓN, Irene DOMÍNGUEZ, Vicente FORNÉ a María J. SABATER. Gold supported on a biopolymer (chitosan) catalyzes the regioselective hydroamination of alkynes. *Journal of Catalysis*

- [online]. 2007, **251**(1), 39–47. ISSN 0021-9517. Available from: doi:10.1016/j.jcat.2007.07.021
- [59] MÜNSTER, Lukáš, Zdenka CAPÁKOVÁ, Petr HUMPOLÍČEK, Ivo KUŘITKA, Bjørn E. CHRISTENSEN a Jan VÍCHA. Dicarboxylated hyaluronate: Synthesis of a new, highly functionalized and biocompatible derivative. *Carbohydrate Polymers* [online]. 2022, **292**, 119661. ISSN 0144-8617. Available from: doi:10.1016/j.carbpol.2022.119661
- [60] MUCHOVÁ, Monika, Lukáš MÜNSTER, Alžběta VÁVROVÁ, Zdenka CAPÁKOVÁ, Ivo KUŘITKA a Jan VÍCHA. Comparison of dialdehyde polysaccharides as crosslinkers for hydrogels: The case of poly(vinyl alcohol). *Carbohydrate Polymers* [online]. 2022, **279**, 119022. ISSN 0144-8617. Available from: doi:10.1016/j.carbpol.2021.119022
- [61] KIM, Ung-Jin, Hyeon KIM, Joon CHOI, Satoshi KIMURA a Masahisa WADA. Cellulose-chitosan beads crosslinked by dialdehyde cellulose. *Cellulose* [online]. 2017, **24**. Available from: doi:10.1007/s10570-017-1528-y
- [62] BELOWICH, Matthew E. a J. Fraser STODDART. Dynamic imine chemistry. *Chemical Society Reviews* [online]. 2012, **41**(6), 2003–2024. ISSN 1460-4744. Available from: doi:10.1039/C2CS15305J
- [63] EGBO, Munonyedi Kelvin. A fundamental review on composite materials and some of their applications in biomedical engineering. *Journal of King Saud University - Engineering Sciences* [online]. 2021, **33**(8), 557–568. ISSN 1018-3639. Available from: doi:10.1016/j.jksues.2020.07.007
- [64] TAMAYO, Laura, Humberto PALZA, Julián BEJARANO a Paula A. ZAPATA. 8 - Polymer Composites With Metal Nanoparticles: Synthesis, Properties, and Applications. In: Krzysztof PIELICHOWSKI a Tomasz M. MAJKA, ed. *Polymer Composites with Functionalized Nanoparticles* [online]. B.m.: Elsevier, 2019 [vid. 2023-11-09], Micro and Nano Technologies, s. 249–286. ISBN 978-0-12-814064-2. Available from: doi:10.1016/B978-0-12-814064-2.00008-1
- [65] VOJDANI, Mahroo a Rashin GITI. Polyamide as a Denture Base Material: A Literature Review. *Journal of Dentistry*. 2015, **16**(1 Suppl), 1–9. ISSN 2345-6485.
- [66] ALI, Asif. Polyamide Syntheses. In: [online]. 2017. Available from: doi:10.1007/978-3-642-29648-2_418

- [67] YI, Chunwang, Zhihan PENG, Huaping WANG, Min LI a Chaosheng WANG. Synthesis and characteristics of thermoplastic elastomer based on polyamide-6. *Polymer International* [online]. 2011, **60**(12), 1728–1736. ISSN 0959-8103, 1097-0126. Available from: doi:10.1002/pi.3140
- [68] GILBERT, Marianne. Chapter 18 - Aliphatic Polyamides. In: Marianne GILBERT, ed. *Brydson's Plastics Materials (Eighth Edition)* [online]. B.m.: Butterworth-Heinemann, 2017 [vid. 2023-11-14], s. 487–511. ISBN 978-0-323-35824-8. Available from: doi:10.1016/B978-0-323-35824-8.00018-9
- [69] BIANCO, B., L. CASTALDO, A. DEL GAUDIO, G. MAGLIO, R. PALUMBO, F. LA CARA, G. PELUSO a O. PETILLO. Biocompatible α -aminoacids based aliphatic polyamides. *Polymer Bulletin* [online]. 1997, **39**(3), 279–286. ISSN 1436-2449. Available from: doi:10.1007/s002890050149
- [70] VÁVROVÁ, Alžběta, Tereza ČAPKOVÁ, Ivo KUŘITKA, Jan VÍCHA a Lukáš MÜNSTER. One-step synthesis of gold nanoparticles for catalysis and SERS applications using selectively dicarboxylated cellulose and hyaluronate. *International Journal of Biological Macromolecules* [online]. 2022, **206**, 927–938. ISSN 0141-8130. Available from: doi:10.1016/j.ijbiomac.2022.03.043
- [71] DŮBRAVOVÁ, Alžběta, Monika MUCHOVÁ, David ŠKODA, Lenka LOVECKÁ, Lucie ŠIMONÍKOVÁ, Ivo KUŘITKA, Jan VÍCHA a Lukáš MÜNSTER. Highly efficient affinity anchoring of gold nanoparticles on chitosan nanofibers via dialdehyde cellulose for reusable catalytic devices. *Carbohydrate Polymers* [online]. 2023, 121435. ISSN 0144-8617. Available from: doi:10.1016/j.carbpol.2023.121435
- [72] MEDŘÍKOVÁ, Zdenka, Petr JAKUBEC, Václav RANC, Aristides BAKANDRITSOS, Josef KAŠLÍK a Radek ZBOŘIL. Carboxymethylcellulose-based magnetic Au or Ag nanosystems: Eminent candidates in catalysis, sensing applications based on SERS, and electrochemistry. *Applied Materials Today* [online]. 2019, **14**, 143–150. ISSN 2352-9407. Available from: doi:10.1016/j.apmt.2018.12.001
- [73] KOZUCH, Sebastian a Jan M. L. MARTIN. “Turning Over” Definitions in Catalytic Cycles. *ACS Catalysis* [online]. 2012, **2**(12), 2787–2794. Available from: doi:10.1021/cs3005264

LIST OF FIGURES

Figure 1: Display of AuNPs colour dependence on their size and shape [12, 15]	8
Figure 2: Reduction of 4-nitrophenol to 4-aminophenol in the presence of NaBH ₄ and AuNPs [27].....	9
Figure 3: Schematic representation of a particle in a dispersion medium and theoretical scheme of the zeta potential [31]	11
Figure 4: Structure of the cellulose unit [43].....	12
Figure 5: Structure of the hyaluronic acid unit.....	13
Figure 6: Structure of chitosan unit [50].....	13
Figure 7: Structure of dextran unit [53].....	14
Figure 8: Structure of alginate unit [57]	14
Figure 9: General scheme of primary oxidation (A), formation of Schiff base between CHO and NH ₂ group (B) and formation of amine bond after reduction of Schiff base (C) [60, 61].....	15
Figure 10: General scheme of secondary oxidation [60].....	15
Figure 11: Synthesis of Polyamide 6 [67].....	16
Figure 12: Scheme of the catalytic device [71]	21
Figure 13: FT-IR spectra for cellulose, hyaluronic acid, dextran, alginate and DAC, DAH, DADXA, DAAL, DCC and DCH derivatives.....	22
Figure 14: Screening study of gold nanoparticles prepared from fully oxidized DCC, UV-VIS spectrometry record, measured zeta potential values, TEM microscope images (white scale bar represents 20 nm) and macroscopic image of prepared solutions	23
Figure 15: Scheme of Au salt reduction mechanism for DCC sample.....	25
Figure 16: Comparison of SERS effect on NAC compound signal using AuDCC, AuDCC-70 and AuDCH samples	26
Figure 17: Catalytic activity of AuNPs investigated for the reduction of 4-NP to 4-AP. On the left, dependence of the decrease in absorbance with time, investigated at a wavelength of 400 nm characteristic of 4-NP. On the right, dependence of ln(c _t /c ₀) on reaction time, calculated value of k and TOF	27
Figure 18: Screening study of AuDAC with different DAC weight concentration, UV-VIS spectrometry record, measured zeta potential and hydrodynamic radius values and TEM microscope images of AuDAC06 sample	27
Figure 19: Image of AuCHIT composite and TEM and SEM images of 3 and 168 h AuCHIT time series samples	28
Figure 20: Stability of the final composite material in a PBS solution of pH 3, 7 and 9.	29
Figure 21: Catalytic activity of AuDAC sample and composite AuCHIT material from AuDAC and chitosan nanofibers	29
Figure 22: UV-Vis spectra with LSPR values for AuDAAL, AuDADXA and AuDAH and their hydrodynamic radius (r _h) values with a polydispersity index (PDI).....	30

Figure 23: Dependence of $\ln(c_t/c_0)$ on reaction time, calculated values of k and TOF of AuDAAL, AuDADXA and AuDAH for catalytic reduction of 4-NP ...31

Figure 24: UV-Vis spectra of starting solutions of AuDAC and AuDAH and spectra of solutions after binding to polyamide and chitosan nanofibers with the amount of AuNPs attached to fibre bodies.....32

LIST OF TABLES

Table 1: Molecular weight of the prepared polysaccharides derivatives, M_w is weight-average molecular weight, M_n is number-average molecular weight, PDI is polydispersity index and DP is the degree of polymerization22

Table 2: Antibacterial activity for composite samples for bacterial strains Staphylococcus aureus CCM 4516 and Escherichia coli CCM 451732

LIST OF ABBREVIATIONS AND SYMBOLS

AL	Alginate	NaClO ₂	Sodium chlorite
AuNPs	Gold nanoparticles	NaIO ₄	Sodium periodate
CHIT	Chitosan	NaOH	Sodium hydroxide
CHO	Aldehyde functional group	NH ₂	Amine functional group
COOH	Carboxyl functional group	NMR	Nuclear magnetic resonance
DAAL	Dialdehyde dextran	OH	Hydroxyl functional group
DAC	Dialdehyde cellulose	PA	Polyamide
DADXA	Dialdehyde dextran	PDI	Polydispersity index
DAH	Dialdehyde hyaluronate	PEG	Polyethylene glycol
DCAL	Dicarboxy alginate	PEO	Polyethylene oxide
DCC	Dicarboxy cellulose	SEM	Scanning electron microscope
DCDXA	Dicarboxy dextran	SERS	Surface-enhanced Raman scattering
DCH	Dicarboxy hyaluronate	STAB	Sodium triacetoxymethylborohydride
DCP	oxidized dicarboxy-polysaccharides	TEM	Transmission electron microscope
DLS	Dynamic light scattering	TGA	Thermogravimetric analysis
DMSO	Dimethylsulfoxid	TOF	Turnover frequency
DO	Degree of oxidation	UV/Vis	Ultraviolet-visible spectroscopy
DXA	Dextran	XRD	X-ray diffraction analysis
FT-IR	Fourier-transform infrared spectroscopy	XRF	X-ray fluorescence analysis
GPC	Gel permeation chromatography	4-AP	4-Aminophenol
HYA	Hyaluronic acid	4-NP	4-Nitrophenol
H ₂ O ₂	Hydrogen peroxide		
LSPR	Localized surface plasmon resonance		
MWCO	Molecular-weight cut off		
M _w	Molecular weight		
NaBH ₄	Sodium borohydride		
NAC	N-acetylcysteine		

LIST OF PUBLICATIONS

Articles in impacted journals indexed on WoS in Science Citation Index Expanded (SCIE)

[1] VÁVROVÁ, Alžběta, Tereza ČAPKOVÁ, Ivo KUŘITKA, Jan VÍCHA and Lukáš MÜNSTER. One-step synthesis of gold nanoparticles for catalysis and SERS applications using selectively dicarboxylated cellulose and hyaluronate. *International Journal of Biological Macromolecules* [online]. 2022, **206**, 927–938. ISSN 0141-8130. Available from: doi:10.1016/j.ijbiomac.2022.03.043

[2] MUCHOVÁ, Monika, Lukáš MÜNSTER, Alžběta VÁVROVÁ, Zdeňka CAPÁKOVÁ, Ivo KUŘITKA and Jan VÍCHA. Comparison of dialdehyde polysaccharides as crosslinkers for hydrogels: The case of poly(vinyl alcohol). *Carbohydrate Polymers* [online]. 2022, **279**, 119022. ISSN 0144-8617. Available from: doi:10.1016/j.carbpol.2021.119022

[3] DŮBRAVOVÁ, Alžběta, Monika MUCHOVÁ, David ŠKODA, Lenka LOVECKÁ, Lucie ŠIMONÍKOVÁ, Ivo KUŘITKA, Jan VÍCHA and Lukáš MÜNSTER. Highly efficient affinity anchoring of gold nanoparticles on chitosan nanofibers via dialdehyde cellulose for reusable catalytic devices. *Carbohydrate Polymers* [online]. 2023, 121435. ISSN 0144-8617. Available from: doi:10.1016/j.carbpol.2023.121435

Full-text contribution to conference proceedings

Preparation of Gold Nanoparticles Using Polysaccharide Dialdehydes and Study of their Catalytic Activity. DŮBRAVOVÁ, Alžběta, Monika MUCHOVÁ, Lenka LOVECKÁ, Ivo KUŘITKA, Jan VÍCHA and Lukáš MÜNSTER. In the NANOCON 2023 conference proceedings.

CURRICULUM VITAE

Personal information

Name: Alžběta Důbravová (Vávrová)
Date of birth: 14th March 1995
Place of birth: Zlín, Czech Republic
Nationality: Czech
Orcid: 0000-0001-5782-0577
Permanent address : Dobrkovice 105
763 07 Dobrkovice
Czech Republic

Email: avavrova@utb.cz
Telephone: +420 731 289 993

Affiliation: Centre of polymer systems
Tomas Bata University in Zlin
Tř. Tomáše Bati 5678
760 01 Zlin
Czech Republic

Education

2019–present Ph.D. student, Nanotechnology and advanced materials,
Tomas Bata University, Zlín, Czech Republic.
2017–2019 MSc. in Chemistry, technology and properties of materials,
Brno University of Technology, Brno, Czech Republic
2014–2017 BSc. in Chemistry, technology and properties of materials,
Brno University of Technology, Brno, Czech Republic
2010–2014 Grammar school and Language school with state language
examination Zlín

Research projects

IGA/CPS/2023/006, IGA/CPS/2022/002, IGA/CPS/2021/002, IGA/CPS/2020/03, RP/CPS/2020/006, OP PIK CZ.01.1.02/0.0/0.0/20_321/0025211, RP/CPS/2022/007, The Czech Science Foundation grant GA23-07361S

Other activities:

Research stay at O'Brien Centre for Science, **University College Dublin**, Ireland, under the supervision of Assoc. Prof. Susan Quinn (October 2022–November 2022)

Research stay at the **University of La Laguna**, Tenerife, under the supervision of Prof. Elena Pastor Tejera (July 2023)

Future research stay at **Hanyang University**, Seoul, South Korea, under the supervision of Prof. Jeong Gil Seo (December 2023–February 2024).

Ing. Alžběta Důbravová, Ph.D.

Příprava nanočástic zlata pomocí oxidovaných polysacharidů

Preparation of gold nanoparticles using oxidized polysaccharides

Doctoral Thesis Summary

Published by: Tomas Bata University in Zlín

nám. T. G. Masaryka 5555, 760 01 Zlín

Edition: published electronically

Typesetting by: Ing. Alžběta Důbravová, Ph.D.

This publication has not undergone any proofreading or editorial review.

Publication year: 2024

First Edition

ISBN 978-80-7678-239-6

